UNIVERSIDAD DE INVESTIGACIÓN DE TECNOLOGÍA EXPERIMENTAL YACHAY

Escuela de Ciencias de la Tierra, Energía y Ambiente

TÍTULO: CARACTERIZACIÓN DE DEPÓSITOS DE CORRIENTE DE DENSIDAD PIROCLÁSTICA ASOCIADOS A LA CALDERA DE CUICOCHA, NORTE DE LOS ANDES ECUATORIANOS.

Trabajo de integración curricular presentado como requisito para la obtención del título de Geóloga

Autor:

Patricia Janeth Rengel Calvopiña

Tutor:

Ph. D. Almeida Gonzalez Rafael

Urcuquí, Julio 2020

Urcuquí, 15 de abril de 2020

SECRETARÍA GENERAL
(Vicerrectorado Académico/Cancillería)
ESCUELA DE CIENCIAS DE LA TIERRA, ENERGÍA Y AMBIENTE
CARRERA DE GEOLOGÍA
ACTA DE DEFENSA No. UITEY-GEO-2020-00008-AD

A los 15 días del mes de abril de 2020, a las 11:30 horas, de manera virtual mediante videoconferencia, y ante el Tribunal Calificador, integrado por los docentes:

Presidente Tribunal de Defensa	Dr. MARTIN MERINO, GERMAN , Ph.D.
Miembro No Tutor	Dra. MANDON CELINE LUCIE , Ph.D.
Tutor	Dr. ALMEIDA GONZALEZ, RAFAEL VLADIMIR , Ph.D.

El(la) señor(ita) estudiante **RENGEL CALVOPIÑA, PATRICIA JANETH**, con cédula de identidad No. **1725202830**, de la **ESCUELA DE CIENCIAS DE LA TIERRA, ENERGÍA Y AMBIENTE**, de la Carrera de **GEOLOGÍA**, aprobada por el Consejo de Educación Superior (CES), mediante Resolución **RPC-SE-10-No.031-2016**, realiza a través de videoconferencia, la sustentación de su trabajo de titulación denominado: **TCHARACTERIZATION OF PYROCLASTIC DENSITY CURRENT DEPOSITS AT CUICOCHA CALDERA VOLCANO, NORTHERN ECUADORIAN ANDES**, previa a la obtención del título de **GEÓLOGO/A**.

El citado trabajo de titulación, fue debidamente aprobado por el(los) docente(s):

Tutor	Dr. ALMEIDA GONZALEZ, RAFAEL VLADIMIR , Ph.D.

Y recibió las observaciones de los otros miembros del Tribunal Calificador, las mismas que han sido incorporadas por el(la) estudiante.

Previamente cumplidos los requisitos legales y reglamentarios, el trabajo de titulación fue sustentado por el(la) estudiante y examinado por los miembros del Tribunal Calificador. Escuchada la sustentación del trabajo de titulación a través de videoconferencia, que integró la exposición de el(la) estudiante sobre el contenido de la misma y las preguntas formuladas por los miembros del Tribunal, se califica la sustentación del trabajo de titulación con las siguientes calificaciones:

Tipo	Docente	Calificación
Presidente Tribunal De Defensa	Dr. MARTIN MERINO, GERMAN , Ph.D.	9,3
Miembro Tribunal De Defensa	Dra. MANDON CELINE LUCIE , Ph.D.	8,9
Tutor	Dr. ALMEIDA GONZALEZ, RAFAEL VLADIMIR , Ph.D.	8,0

Lo que da un promedio de: **8.7 (Ocho punto Siete)**, sobre 10 (diez), equivalente a: **APROBADO**

Para constancia de lo actuado, firman los miembros del Tribunal Calificador, el/la estudiante y el/la secretario ad-hoc.

Certifico que *en cumplimiento del Decreto Ejecutivo 1017 de 16 de marzo de 2020, la defensa de trabajo de titulación (o examen de grado modalidad teórico práctica) se realizó vía virtual, por lo que las firmas de los miembros del Tribunal de Defensa de Grado, constan en forma digital.*

RENGEL CALVOPIÑA, PATRICIA JANETH
Estudiante

Patty Rengel

Dr. MARTIN MERINO, GERMAN , Ph.D.
Presidente Tribunal de Defensa

MARTIN MERINO GERMAN - 12780762F

Firmado digitalmente por MARTIN MERINO GERMAN - 12780762F
Nombre de reconocimiento (DN): c=ES, serialNumber=IDCES-12780762F, givenName=GERMAN, sn=MARTIN MERINO, cn=MARTIN MERINO GERMAN - 12780762F
Fecha: 2020.06.08 16:24:12 -05'00'

UNIVERSIDAD YACHAY TECH

Dr. ALMEIDA GONZALEZ, RAFAEL VLADIMIR , Ph.D.
Tutor

RAFAEL VLADIMIR ALMEIDA GONZALEZ

Digitally signed by RAFAEL VLADIMIR ALMEIDA GONZALEZ
DN: c=EC, o=BANCO CENTRAL DEL ECUADOR, ou=ENTIDAD DE CERTIFICACION DE INFORMACION-ECIBCE, l=QUITO, serialNumber=0000317770, cn=RAFAEL VLADIMIR ALMEIDA GONZALEZ
Date: 2020.04.15 13:55:09 -05'00'

Dra. MANDON CELINE LUCIE , Ph.D.
Miembro No Tutor

Firmado electrónicamente por:
CELINE LUCIE

TERÁN ROSALES, ANDREA YOLANDA
Secretario Ad-hoc

ANDREA YOLANDA TERAN ROSALES

Firmado digitalmente por ANDREA YOLANDA TERAN ROSALES
Fecha: 2020.05.05 13:47:22 -05'00'

AUTORÍA

Yo, **Patricia Janeth Rengel Calvopiña**, con cédula de identidad 1725202830, declaro que las ideas, juicios, valoraciones, interpretaciones, consultas bibliográficas, definiciones y conceptualizaciones expuestas en el presente trabajo; así cómo, los procedimientos y herramientas utilizadas en la investigación, son de absoluta responsabilidad de el/la autora (a) del trabajo de integración curricular. Así mismo, me acojo a los reglamentos internos de la Universidad de Investigación de Tecnología Experimental Yachay.

Urcuquí, Julio 2020.

Patty Rengel

Patricia Janeth Rengel Calvopiña

CI: 1725202830

AUTORIZACIÓN DE PUBLICACIÓN

Yo, **Patricia Janeth Rengel Calvopiña,** con cédula de identidad 1725202830, cedo a la Universidad de Tecnología Experimental Yachay, los derechos de publicación de la presente obra, sin que deba haber un reconocimiento económico por este concepto. Declaro además que el texto del presente trabajo de titulación no podrá ser cedido a ninguna empresa editorial para su publicación u otros fines, sin contar previamente con la autorización escrita de la Universidad.

Asimismo, autorizo a la Universidad que realice la digitalización y publicación de este trabajo de integración curricular en el repositorio virtual, de conformidad a lo dispuesto en el Art. 144 de la Ley Orgánica de Educación Superior

Urcuquí, Julio 2020.

Patty Rengel

Patricia Janeth Rengel Calvopiña

CI: 1725202830

“El mayor desafío que enfrentan nuestros países de cara al futuro como naciones con doscientos años de independencia es la educación. Un tema estratégico por relacionarse directamente con el desarrollo nacional, con la construcción de la sociedad en su conjunto.

La educación no consiste sólo en la formación de capital humano para el mercado. En ella trabajamos con las esperanzas de realización de los jóvenes: promesa y futuro abierto que no puede verse defraudado. La educación es una responsabilidad del ser humano para con el ser humano, es la responsabilidad de forjar valores y principios, y también de otorgar las posibilidades para transitar por el camino del desarrollo sin limitaciones.”

Víctor L. Pérez Vera.
Salón de Honor de la Universidad de Chile
Santiago, Marzo 11 de 2008

Dedicatoria

I want to dedicate this work to my mom *Marina Alicia* and sister *Graciela Lucia* that, during all my career, support me with the most beautiful details. In the universe, you are my best example of unconditional love. I want to thank my dad *Francisco Hermogenes*, grandparents *Marina*, *Gonzalo*, *Carmelina* †, and *Alberto* †, and in general, all my family that always have been there sending good vibes.

I want to give a big thank you to each one of my friends at Yachay Tech. My best friends, the geomates, and roomies. Every coffee, asadito, party, or in general conversation is part of the best stage in my life until now. Last but not least my boyfriend Sherald; I love you,your mind and the way that your smile destroys the routine.

We all transform our country day by day. Let’s keep dreaming in a better future!

Patty J.

Aknowledgment

This thesis work represents the first stage in my career as a researcher in the field of earth science. Then, I am very (very) grateful to my advisors Rafael Almeida (Yachay Tech), Matteo Roverato for their patience and motivation to help me successfully finish this study; Maurizio Mulas (ESPOL) for his support during the granulometry study and of course Michelle Villalta, that loves volcanos even more than me; German Merino is thanked for sharing his stratigraphy and sedimentology knowledge and his constructive comments on the hardest stage in this work, and a big thank to the best assistant of the geology faculty Andrea Terán that always support us making things and processes easier. I want to thank every professor in the career Luke, Patri, Elisa, Celine, Jorge, Yaniel, Anna, Isma, Edwin, Paul, Luis Felipe, Alejandra, Alyssia, Bryan, Uwe, that not only shared their knowledge in earth science moreover they shared friendship, passion, and enthusiasm to be better persons every day and love the science.

Patty J.

Resumen

La caldera de Cuicocha es el centro eruptivo más joven en el Complejo Volcánico Cotacachi-Cuicocha, y su historia eruptiva es poco conocida. La caldera de Cuicocha ha experimentado dos episodios eruptivos con corrientes de densidad piroclástica asociadas y el emplazamiento de depósitos de ignimbrita. El primer evento es responsable de la destrucción del Domo Cuicocha, la formación de la caldera (4100 ± 0.15 BP) y un depósito de ignimbrita asociado de 4.1 km3. Mientras tanto, el segundo depósito de piroclastos es una reactivación en el complejo caracterizado principalmente por flujos de piedra pómez (3900 ± 0.15 BP) y es la etapa previa a la formación de las cuatro cúpulas intracaldera actuales, y su ignimbrita asociada tiene 0.8 km3.

Este trabajo considera los ignimbritas que afloran en cinco canteras, que se encuentran a 6 – 7 km al sureste de la caldera para análisis de variabilidad horizontal y vertical a través de estratigrafía, sedimentología y también catorce muestras granulometría, y componentes del PDC. De esta manera, los procesos relacionados con el transporte y el emplazamiento en las unidades reflejan que: las unidades A y C consisten en depósitos volcánicos primarios con facies masivas, estas unidades fueron depositadas progresivamente por un flujo concentrado inestable visible sobre toda el área estudiada; la unidad B consiste en una secuencia de facies estratificada y estratificadas difusa que tiene un grosor variable y registra un flujos estables e inestable de origen primario y secundario, depositados por la agregación progresiva o mecanismo de depósito *en masse*. Ambas unidades reflejas miembros de los extremos del espectro de flujos piroclasticos. Finalmente, se ha observado una baja variabilidad vertical en parámetros y componentes estadísticos en las unidades masivas A y C.

Palabras clave: Caldera Cuicocha, PDC, ignimbritas, estratigrafía, facies, granulometría, componentes.

Summary

Cuicocha caldera is the youngest eruptive center in the Cotacachi-Cuicocha Volcanic Complex, and its eruptive history is poorly known. Cuicocha caldera has experienced two eruptive episodes with associated pyroclastic density currents and emplacement of ignimbrite deposits. The first event is responsible for the destruction of Cuicocha Dome, the formation of the caldera (4100 ±0.15 BP), and an associated ignimbrite deposit of 4.1 km^3. Meanwhile, the second pyroclastic deposit is consequence of a reactivation in the complex characterized mainly by pumices flows (3900 ± 0.15 BP) and is the stage before the formation of the current four intra-caldera domes, and its associated ignimbrite has 0.8 km^3.

This work considers the ignimbrites that outcrop at five quarries, which are located 6km to the southeast of the caldera, and fourteen samples for horizontal and vertical analysis of variability through stratigraphy, sedimentology, and granulometry, and components of the PDC. In this way the processes related to the transport and emplacement in the units reflect that: Units A and C consists of primary volcanic deposits with massive facies, units A and C that were deposited by a concentrated unsteady flow progressively aggraded over all the studied area; unit B of consist of stratified and diffuse stratified facies sequence has a variable thickness, and record a successive unsteady and steady flow of primary and secondary origin, deposited by progressive aggradation and *en masse* mechanim. The massive ignimbrites are a consequence of a concentrated PDC, while the stratified layer from a surge or dilute PDC, both are end members of the current spectrum. Finally, it has been observed low vertical variability in statistical parameter and components in the massive Units A and C.

Keywords: Cuicocha Caldera, PDC, ignimbrites, stratigraphy, facies, granulometry, components.

CONTENT

TABLE OF FIGURES

TABLES

Chapter 1: Introduction

The Cuicocha caldera is the youngest volcanic emission center of Cotacachi-Cuicocha Volcanic Complex (CCVC) located in the northern Ecuadorian Andes in Imbabura Province. Five emission centers constituted the CCVC: a single stratovolcano called Cotacachi, which is the oldest, and four domes: Muyurcu, Loma Negra, Peribuela, and Cuicocha. Cuicocha caldera was originated after the explosive eruption of Cuicocha dome ~4100 years ago (von Hillebrandt, 1989; Fig. 1). This eruptive process produced a pyroclastic density current (PCD), and later the second episode of volcanic activity produce a second PDC. This thesis project aims to characterize the mentioned deposits to support interpretations about the transportation and emplacement conditions of the PDC's during and after the caldera-forming event (CFE).

The PDC's deposited in the surrounding areas has been broadly described in the literature

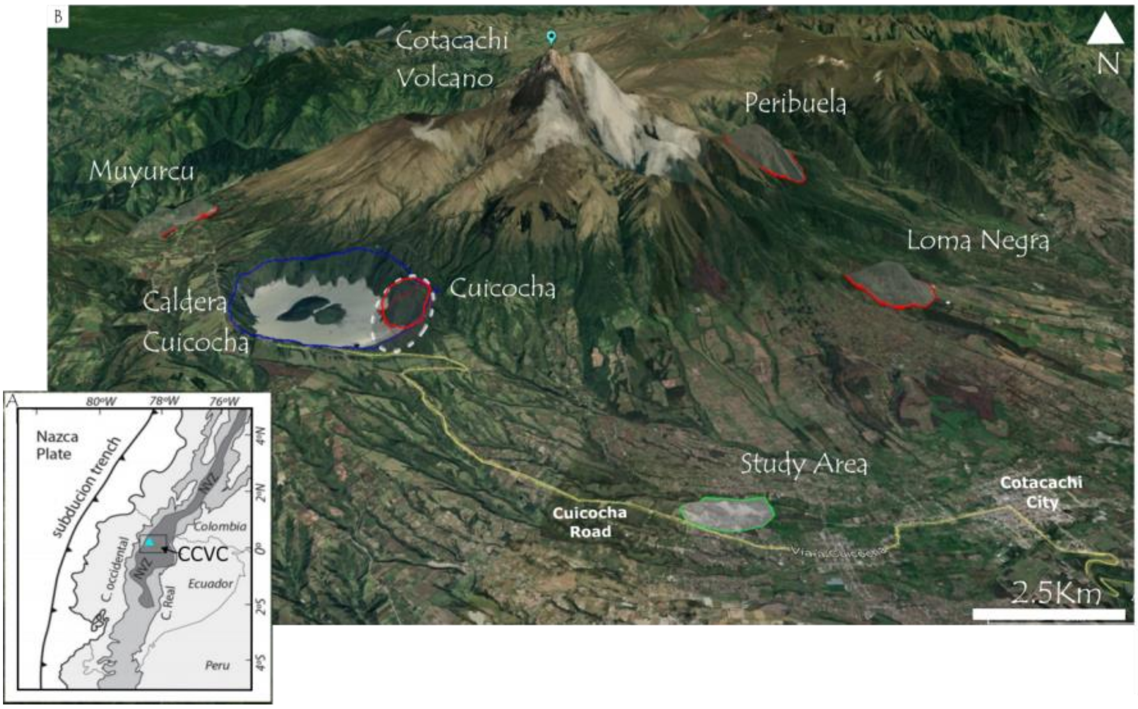

Fig. 1 A) Location of CCVC in the northern volcanic zone (NVC)(Modified from: Roverato, 2018) B)Panoramic view from Google Earth that shows the CCVC (vertical exaggeration 1.8X). The highest point of Imbabura province is the peak of Cotacachi volcano (blue dot 4.944 m.a.s.l.; 0°21'38.20"N, 78°20'54.70"W). The red polygons are surrounding the domes: Muyurco, Peribuela, Loma Negra, and the remains of Cuicocha Dome. The white dotted line limits the perimeter of what was Cuicocha dome before its explosion (von Hillebrandt, 1989). The studied area is the green polygon at the bottom right of the map, and the blue one is Cuicocha Caldera.

(Mueller et al., 2011; Walker, 1971; Walker, 1983; Druitt & Sparks, 1984; Cashman, &

Giordano, 2014) as ignimbrite. These deposits can develop different textural and lithological features known as facies, which besides other physical features and geometrical relations, correlation, grain size distribution, and components, characterize the deposit. Here I applied methods from stratigraphy, sedimentology, and volcanology to describe in detail the distribution, sequence, and sedimentary features in the deposit at 6km from the caldera and the granulometry and components of the massive facies.

The description of volcanic processes of any nature, including transport and deposition in volcanic arcs above subduction zones, is an essential aspect of volcanology research (Pardo, 2012). The characterization of a PDC will support civil society and governments (von Hillebrandt, C. 1989) to develop all types of volcanic information for the inhabitants around including hazard assessment or risk assessment project.

Cuicocha is peculiar because it is the emission center of the most recent volcanism in the CCVC, and the studied area (and its surrounding) is considered active. Furthermore, there is a central lake contained inside the caldera (Fig. 2). These facts motivate a better understanding of the volcanic history of the region to anticipate the behavior of CCVC in case of new volcanic activity. Additionally, no information for the citizens, especially those in the surrounding of the caldera, could be produced without exhaustive scientific studies of the sites. Then, it is clear that a compilation of available and new information is valuable to have new interpretations of volcanic deposits and to keep getting closer to ensuring appropriate information to act intelligently at any time when decisions about volcanic activity must be made.

Besides, Cuicocha caldera lake and, in general, the whole CCVC is considered one of the major tourist attractions in Imbabura province, that recently April 2019 was declared a new UNESCO Global Geoparks (UNESCO, 2019). Moreover, Cuicocha is considered a sacred place for indigenous communities in Imbabura (Fig. 3). All this makes Cuicocha an outstanding attraction for citizensm and at least 211.413 people visited the caldera in the last year (Cadena, A. 2020). Then, as required by UNESCO Geoparks Guidelines, new insights into its geological origin, geological features, and current behavior are a prime concern to preserve the title awarded by UNESCO.

Fig. 2 Picture of Cuicocha Caldera taken at 0°18'46.8"N 78°22'12.5"W. Courtesy of Daniel Piedra. The caldera (3.5 x 2.7 km) has an oval shape and has two islands formed by four intra-caldera domes located in the middle of the lake. The left intra-caldera dome is named Yerovi (south and north), and the right dome is Teodoro Wolf (south and north).

Currently, the information about this place is scarce. Most of the information available about the volcanic history of Cuicocha caldera is not published neither the results of research and interpretations. Sadly, this means that all that we know about Cuicocha remains hidden from the community in libraries. Two authors worked previously in the physical volcanology field. The first one is a master's thesis work by Christa Glee von Hillebrandt Mayo (1989) titled "Geo-volcanic Study of Cuicocha - Cotacachi Volcanic Complex and its Implications, Imbabura Province" completed at the Escuela Politécnica Nacional (EPN) of Quito. The second is another master's thesis by Abigail Pidgen (2014), "Cuicocha Volcano, Ecuador: Reconstruction of major explosive phases through investigation of associated pyroclastic deposits" completed at Oxford University in England.

Notably, von Hillebrandt (1989) obtained new and significant information about the stratigraphy around the CCVC, providing detailed stratigraphy, and the only available dates of the volcanic events. Besides that, the study also provided information about the eruptive centers and their eruptive styles, geochemical composition of the volcanic products, hazard maps, volcanic risk assessment, and a geothermal model. This work is the first that describes, and defines the eruptive story of the CCVC, which includes at least four eruptive stages.

Fig. 3 Ritual ceremony on the Sacred Path at Cuicocha Caldera, taken at 0°17'34.5"N 78°21'38.7"W. Part of the Cotacachi-Cayapas, Ecuador National Park. Retrieved from: https://es.unesco.org/galleries/imbabura-unesco-global-geopark-ecuador

Further, Pidgen A. (2014) employed grain size analysis, vesicularity studies, and glass chemistry to understand magmatic, transport and deposition processes of PDC's that happened at the major explosive phases approximately 3.1 ka BP and 2.9 ka BP. Additionally, the author compared her interpretations with analogous eruptions around the world. The author states, as well, the importance of understanding Cuicocha past eruptions in order to act assertively during future volcanic activity.

The current thesis work aims to compile the most information available and provide a new stratigraphic description and correlation of the pyroclastic lithofacies in the deposits in order to contribute to the understanding of the transport mechanism of the different eruptive stages of Cuicocha caldera volcano. This work integrates textural and components observations with grain size analysis, for a new complete characterization of the deposit, which contributes to the knowledge of this active caldera volcano.

Chapter 2: Literature Review: volcanism, calderas and pyroclastic deposits

Calderas constitute the most forceful and hazardous type of volcanoes for the environment and people living in the surrounding areas (Acocella, 2015). CFE's have produced some of the major volcanic events ever described on Earth (Cashman & Giordano 2014). Therefore, the understanding of this type of eruptions is critical not only for academic purposes but also from a hazards point of view. Understanding the CFE of Cuicocha Caldera requires an introduction of important topics regarding explosive eruptions, including volcanism in subduction zones, explosive eruptions, and pyroclastic deposits.

The eruptive style and frequency of volcanic events at subduction zones depend on the volume and type of magma generated by the mantle/crust melting. Along the Pacific Ring of Fire and specifically in the subduction zone located along western South America, the convergent tectonic setting of the oceanic lithosphere of Nazca plate subducting beneath the continental lithosphere of South American plate is responsible for volcanism. As water released during dehydration of the downgoing Nazca plate is added into the mantle wedge, the solidus temperature of the mantle is lowered, allowing the melting of these hydrated rocks (Stern, 2004; Hall et al., 2008).

The internal magma conditions (i.e., volatile content, density, composition) determine the type of eruption: explosive or diffusive. CFE corresponds to an explosive type eruption, which is a result of fractional crystallization of the magma. The explosive magmatic eruptions produce rapid ex-solution and expansion of dissolved volatiles, due to their fast decompression. These conditions lead to the conversion of potential energy into kinetic energy resulting in an explosive eruption and associated phenomena such as crater formation, tephra emission, acoustic and seismic perturbation, volcanic edifice collapse and caldera collapse (Pardo, 2012).

An explosive eruption has its origin in the transformation of the rising liquid magma with crystals and dissolved gas bubbles into a gas phase with liquid drops and solid particles. Magmatic explosive eruptions produce rapid ex-solution and expansion of dissolved volatiles, due to the abrupt reduction of confining pressure. CFE has a standard model, the most popular and accepted. The standard model of CFE describes calderas as a topographic depression, whose subsidence achieve few km and diameter usually have large dimensions >10km, and are formed during or shortly after a major eruption because of the vertical collapse of the caldera floor within a partially emptied magma reservoir (Acocella, 2007, 2015). The system operates in 4 key steps: the transition from rest to unrest, eruption initiation, destabilization, and collapse.

During the first part of a CFE, and the transition from rest to unrest, the magma in the magmatic chamber progressively cools from the margin inward, and the crystals settle because of gravity. This process is named fractional crystallization. Unrest is the stage where the caldera modifies its behavior from a non-eruptive state to more active conditions, which may lead to an eruption (Fig. 4). Unrest is associated with an incrementing seismic activity, changes in microgravity, surface deformation, gas emissions, and surface temperature anomalies, and they can continue even during the eruptive stage (Cashman & Giordano, 2014; Sigurdsson et al., 2015).

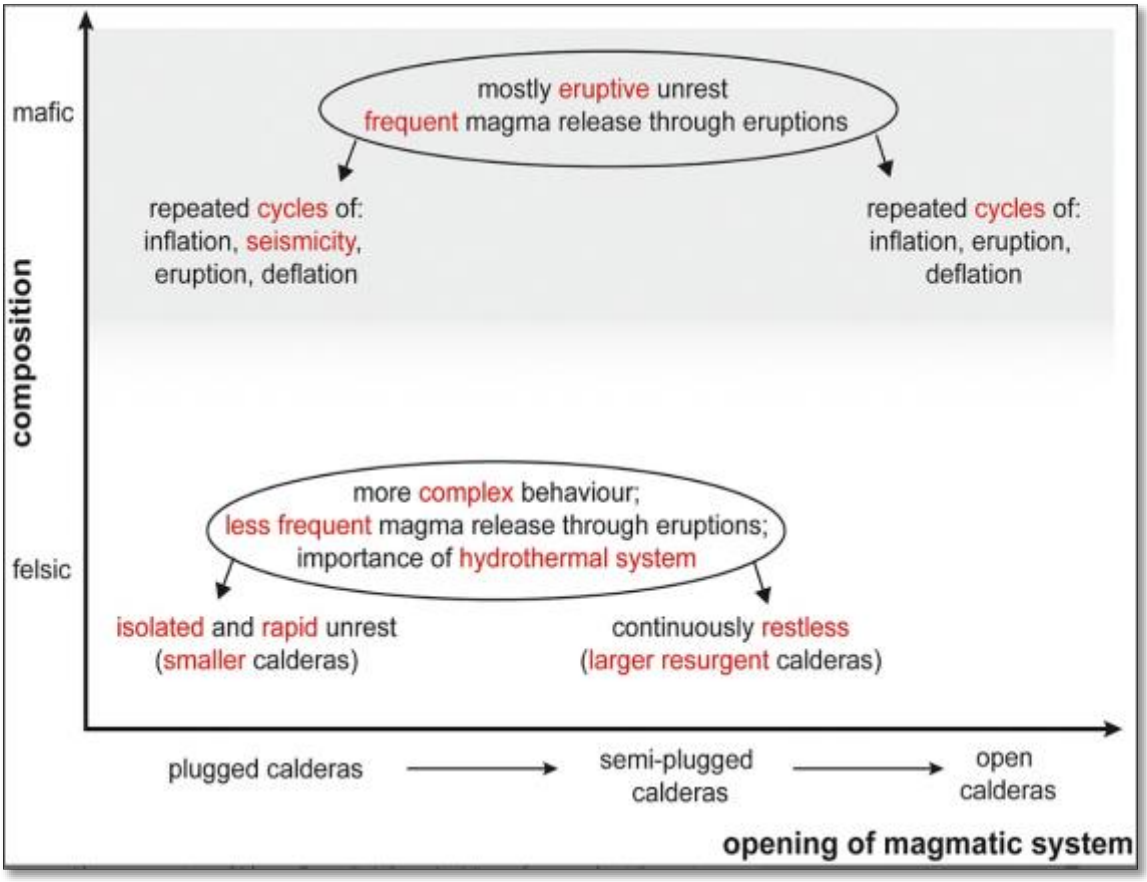

Fig. 4 Summary of the types of unrest as a function of the composition of magma (mafic versus felsic) and the condition of the volcanic conduit (plugged, semi plugged, or open). From: Acocella, 2015.

The volcanic activity can be intermittent or continuous and can continue from minutes like in Mount Saint Helens in the USA, to years as in Reventador Volcano in Ecuador. If the eruption starts, the magmatic chamber will progressively empty and, at the same time, emit several volcanic products such as lava, PDC, ash plumes, and others. Vast volumes of fractionated magma can be ejected in the form of ash volcanic plumes and pyroclastic density currents. In consequence, the partially emptied magma chamber does not support the weight of the overlying column resulting in the collapse and formation of a caldera (Cashman & Giordano, 2014; Sigurdsson et al., 2015).

PDC and volcanic plumes are a mixture of solid particles and gas that travel downslope under the influence of gravity. The ratio between the two components (i.e., solid and gas) defines the type of flow. The currents (flow) vary on a spectrum between concentrated (solid-dominated) PDC and dilute (fluid-dominated) PDC. The PDCs flow down the flanks of volcanos destroying all in the route and depositing hot ignimbrites. Ignimbrites are characterized by poorly sorted ash or tuff matrix, variable components fraction, and unimodal size distribution (Sulpizio, 2014).

The characteristic features can varies horizontally and vertically because of transport and depositional mechanism. On one hand, PDCs move in direct contact with the ground. The ground surface is continuously changing because of the deposition of previous parts of the PDC's. The changing surface constitutes a transition zone named flow boundary zone. On the other hand, some sedimentary structures could also be formed by the deposition style of the PDC.

The deposition types are classified around two end members (1) grain by grain deposition or (2) *en masse*, and both types can be discontinuous or stepwise if is progressive or en masse type if the current is steady and freeze a whole material body. The type depends on the concentration of particles and rates of sedimentation. In this way, extensive ignimbrites show progressively aggradation and deposition, while en masse freezing is more probable with small volume PDC. Each one of them produces, or not, sedimentary structures that support the differentiation of ignimbrites deposits and it is a potent tool to understand the emplacement mechanism and transport (Sulpizio, 2014).

Chapter 3: Geological Framework

Cuicocha caldera is part of the Cotacachi - Cuicocha Volcanic Complex (CCVC) and is located in the western cordillera in the northern Andes (Fig. 5). The Andes are a continuous mountain chain along the west margin of South America formed by the subduction of the Nazca plate beneath the South American plate. According to Stern (2004), the Andean cordillera has an extension of more than 7,500 km and develops from the Caribbean Coast in the north to Cape Horn in the south. The Andean Cordillera is divided into three segments: The Northern (12ºN-5ºS), the Central (5º-33ºS), and the Southern (33-56ºS) active volcanic zones. The northern Andean zone is located in Ecuador and Colombia, trending northeast-southwest. In Ecuador, the Andes are defined by two cordilleras: The Eastern Cordillera and Western Cordillera, with the Inter-Andean Valley in the middle (Stern, 2004).

The abundance and diversity of Ecuadorian volcanism (Hall et al., 2008) are also represented in CCVC. The volcanic complex is delimited by the Chachimbiro volcanic complex at the north, Fuya Fuya-Mojanda volcanoes in the south, while at the southwest is Imbabura volcano and at the east flows the Ambi river (Fig. 5). According to von Hillebrandt (1989), the oldest edifice in Cotacachi, which was active in the middle Pliocene, meanwhile, in chronological order, the followers are Muyurcu, Loma Negra, Peribuela, and Cuicocha. The chronological order was defined based on the K/Ar dating for Cotacachi and Loma Negra and stratigraphic correlations of the deposits for Muyurcu, Peribuela, and Cuicocha (von Hillebrandt, 1989; Almeida, 2014).

Cuicocha is an active caldera at 3072 m.a.s.l., which formed as a consequence of the explosive eruption of the previous Cuicocha dome that collapsed at 3.1 ka. The remains of Cuicocha dome are located at the NEE limit of the crater rim (Fig.1). The caldera is an oval depression with a width of 3,5 km in the major axis and 2,7 km in the minor axis partially filled with a lake. Four domes have grown inside the caldera. They are south Yerovi, north Yerovi, south Wolf, and north Wolf (von Hillebrandt, 1989).

The Geophysics Institute of the Escuela Politecnica Nacional (Instituto Geofísico de la EPN) is continuously monitoring the seismicity, deformation, and CO2 emissions of the caldera volcano with a network composed of 4 seismic stations and two high precision GPS for deformation, three accelerometers, and one CO2 gas measurement apparatus (Córdova et al., 2019; IG-EPN, 2019; Fig. 6).

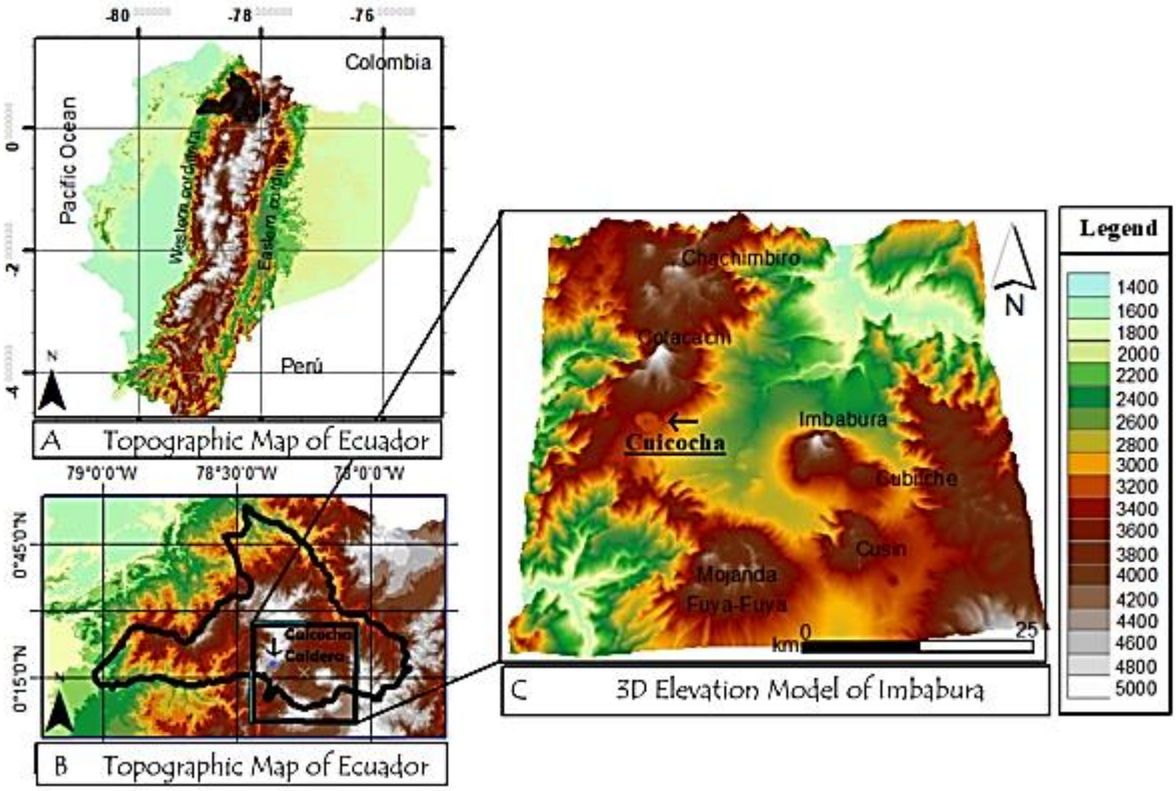

Fig. 5 Topographic map to locate the studied zone. A) Ecuador topographic map in the upper left. The western and eastern cordilleras could be identifying in white color. The province of Imbabura is marked in black. B)Imbabura province topographic map in black. Tthe blue dot is Cuicocha Caldera. Finally, C) 3D elevation model with the major volcanos including CCVC at the right side of the figure.

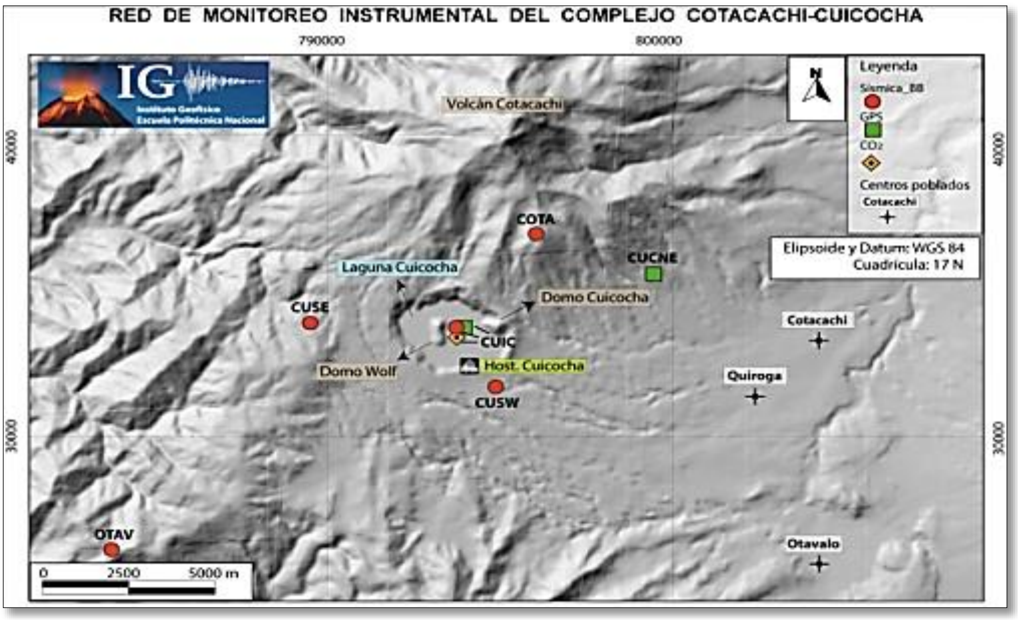

Fig. 6 Monitoring Network at Cuicocha Cotacachi Volcanic Complex. The image shows broad band seismometer, GPS and CO2 apparatus. Taken from: Red de monitoreo CUICOCHA

3.1 Previous works on Cuicocha caldera

Both von Hillebrandt (1989) and Pidgen (2014) studied the stratigraphy and sedimentology of the deposits that are surrounding the caldera. The stratigraphic sequences of both authors are present in Figure 7. Besides describing the eruptive history of Cuicocha Caldera for the first time, von Hillebrandt (1989) also describes the emplacement of the pyroclastic deposits and provides the only dates available for volcanic material from Cuicocha, and years after Pidgen also support some of the information and propose some complements in the eruptive history.

The story of Cuicocha starts with the growth of a dome (Cuicocha). Naturally, the domes are composed of highly viscous lavas; consequently, the degassing process and inner flow of volcanic material were partially or blocked by the dome. According to von Hillenbrandt (1989), the original Cuicocha dome had had a diameter of 1,5km. Nowadays, only a small part of this original dome is preserved in the southern part of the caldera, as Figure 1 shows. Following this, there was a reactivation of the CCVC, which destroyed the dome depositing a block and ash flow in a radio of 1 km and depositing a PDC of 4,1 km^3. Then, new volcanic activity constructed a new dome, which was destroyed due to a new explosive eruption and once again deposited a new PDC of 0,8 km^3. Finally, the domes that nowadays exist inside the caldera start growing. The mentioned PDC deposits are connected to the periods of activity and unrest in this part of the CCVC and are the main object of study in this thesis work.

The stratigraphic reconstructions in both works describe a basement made of Imbabura fine ash, apparently from a fall, and Cangahua (volcanic loess common in Ecuador) (Iriondo & Kröhling, 2007). This unit is called RT in von Hillebrandt (1989) and does not have a name in Pidgen (2014). Above the basement, some variations between both were identified, and will be described. Von Hillebrandt (1989) describes four main units in the deposits D, C, B, and RT (from bottom to top) with a total thickness of 40 m (Fig 7a). Unit D contains grey blocks of lithics in a collapse lava flow deposit associated with the partial destruction of Cuicocha dome. Unit C corresponds to massive PDC deposits from the volcanic activity that destroyed the dome and unit B is composed of cross stratified lapilli and soil at the upper limit and represents the second eruptive activity. In common, Pidgen (2014) also focuses her work on the deposits associated with the first and second reactivation in Cuicocha. Her stratigraphy describes three units: 1, 2, and 3, with a total thickness of 34 m (Fig. 7b). The massive layers associated with pyroclastic flows in the first reactivation correspond to unit 1. Furthermore, unit 2 is a stratified sequence related to the second eruption. Finally, unit 3 is made a transition layer to the soil of the volcanic material deposited by the second eruptive activity.

Finally, the work of von Hillebrandt (1989) and Pidgen (2014) states the following eruptive history model with four stages, which is illustrated in Figure 8.

1) The formation of Cuicocha dome that began at 40 ka, and ended when the main CFE took place (3.1ka ±0,15), and partially destroying the dome and depositing a voluminous PDC.
2) The volcanic activity continues, and a small dome grew; at the same time, the new caldera was partially occupied with water.
3) A new phase of explosive activity occurs (2.9 ka± 0,15), destroying the new dome, and depositing a PDC with evidence of phreatomagmatic explosions.
4) The new dome-building phase forms the four domes inside the caldera

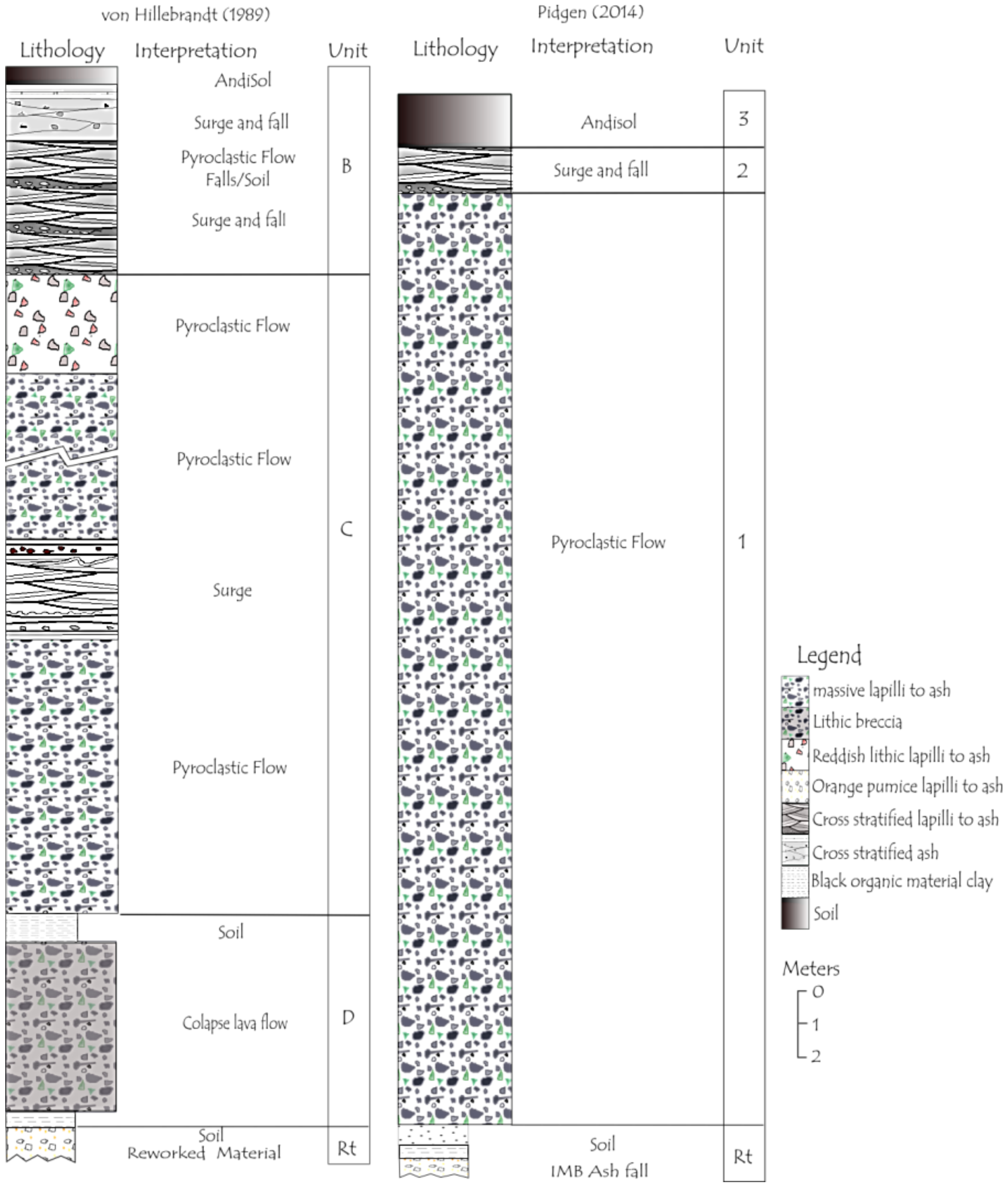

Fig. 7 Stratigraphy associated to the volcanic evolution of Cuicocha. On the left, stratigraphy units: B, C, D, RT from von Hillebrandt (1989). Stratigraphy units from Pidgen (2014) (1, 2, 3) on the left.

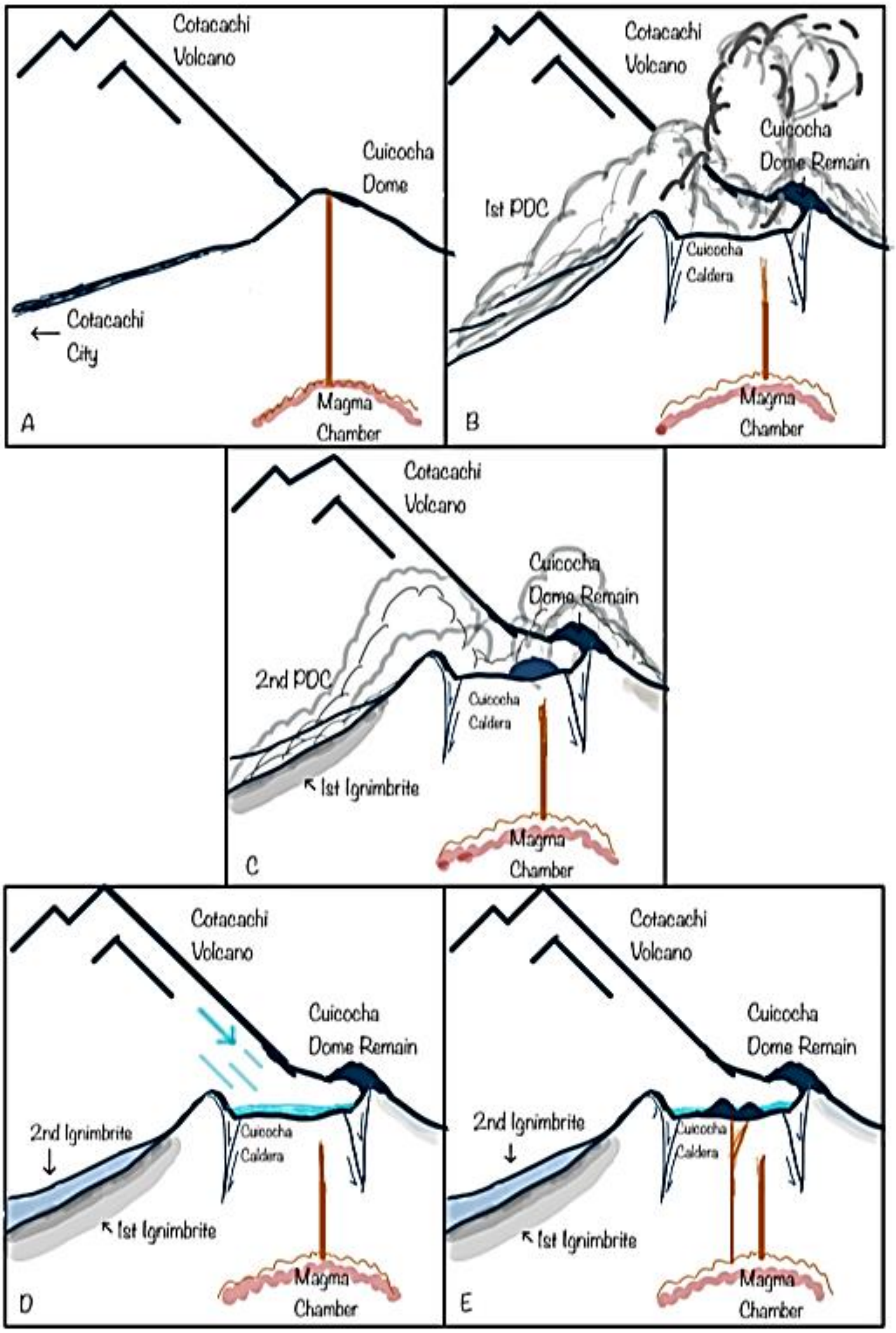

Fig. 8 Cuicocha eruptive history based on von Hillebrandt (1989) and Pidgen (2014) studies. A) Construction of Cuicocha dome on one flank of Cotacachi volcano. B) CFE that destroys Cuicocha dome and produces a PDC depositing the first ignimbrite. C) Filling of the newly formed caldera with water. D) New eruptive phase producing the second ignimbrite. E) Growth of four intra-caldera domes. The graph is not to scale.

Chapter 4: Methodology

4.1 Stratigraphy

Several field campaigns were carried out in the study area to describe in detail the deposits and outcrops to produce stratigraphic columns and correlations. Considering that the predominant direction of the PDCs was toward SE, because of the topography (Pidgen, 2014), we concentrated our campaigns in the deposits located 5km SE from the emission center. Ten stratigraphic columns labeled from I to X have been produced as the result of the field campaigns. Also, 14 samples of 1kg each, were taken as part of the sedimentological studies of the ignimbrite and were used to carry out granulometry and components analysis (Fig. 9).

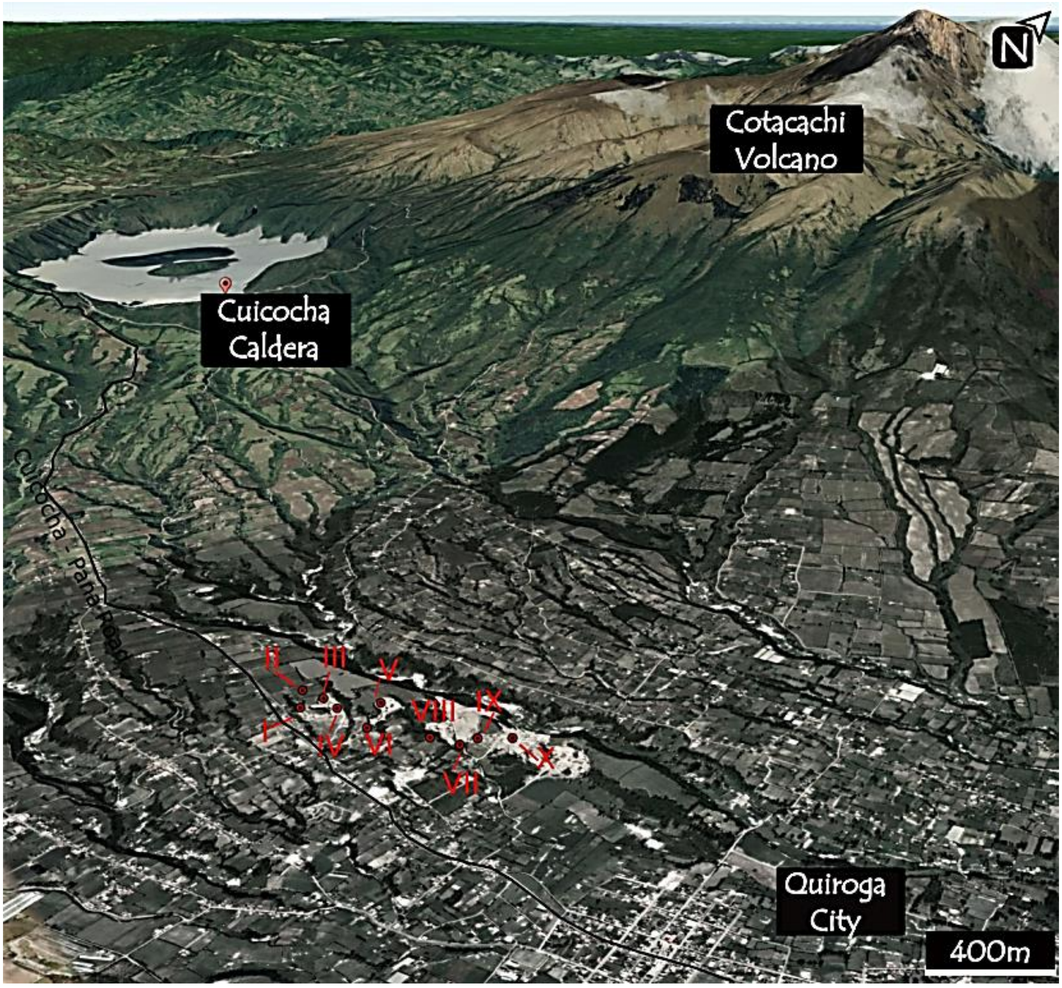

Fig. 9 This oblique view from Google Earth shows the location and the distribution of outcrops (I-X) for stratigraphic columns.

The five quarries in the study display thicknesses from 4 to 15m. The stratigraphic columns represent the sequence of volcanic-sedimentary material that outcrops in the study area and its lithology. The description of the lithology has been done based on textural features, components, sorting, stratigraphic features, and roundness. Finally, constant relationships among the lithologies support a classification of groups of lithology or units. The stratigraphic columns in this work support the evaluation of horizontal variability in the deposits located at 6km from the caldera to the SE. This distribution is spacially restricted and does not allow an assessment of changes from proximal to the distal sites to the caldera.

I should highlight the easy accessibility to the quarries and also the excellent exposure of outcrops. Nevertheless, a drawback in the working area is the mining activity that is continuously changing the outcrops. For example, column IX was exposed towards the end of the fieldwork campaign, and this means that the previous configuration in this side has disappeared. Then, even when some outcrops are vanishing, many others will be exposed in the future for additional research.

The criteria applied here to classify the units corresponds to that suggested by Branney & Kokelaar (2002):

1. Tracing of individual beds/ laminations to define places with invariant thicknesses and grain sizes, areas with thickening and/or coarsening vs. topographic changes.
2. Correlating individual beds and laminations define areas with regular thickness and grain-size variations.
3. Tracing lateral gradations that change into stratified and cross-stratified layers.
4. Detection of abrasion in clasts during transport.

4.2 Particle size analysis

The granulometry fraction corresponds to the percentage of a specific size over the total percentage. The statistical parameters are indicators of origin, transport mechanism, associated energy, and sedimentary environment (Inman, 1952; Folk & Ward 1957; Walker, 1971). The sampled PDC deposits contain various types of pyroclastic fragments of different sizes, where clasts are mostly supported in a fine-grained matrix. The grain size classification used here is volcanological for pyroclastic deposits (ash, lapilli, bombs/blocks), while the volcanoclastic deposits are classified using the sedimentary scale (sand, gravel cobble, boulder) (Roverato, 2013). The granulometry studies include 2 methods, one for coarse ($>-4\varphi$) and medium grain deposits (5φ to -4φ) and another for fine-grain deposits ($<5\varphi$).

First, the samples were heated to 80 °C for 3 hours in metallic containers to dry them out completely. In order to obtain the density of the deposit, we need to obtain the mass and the volume. The mass was obtained by weighing each sample three times. The volume of the measuring cup is also taken into account, so the mass divided by the volume provides an approximate estimate of density of the deposit at the point where the sample was taken. Sieving was carried out in two steps: one sieving group from -4φ to 0φ, and the other from 1φ to 4φ, both with intervals of 1φ. Each sieving column was subject to 5 minutes of vibration in a Retsch Sieve Shaker AS 200. The content of each sieve was measured in an analytical balance and the content stored in labeled plastic bags (Fig. 10).

Finally, the fraction of the remaining material (<4φ, fine fraction) was analyzed in a Horiba LA-300 laser scattering particle size distribution analyzer for which a distribution between 4φ to 11φ was obtained with an interval of 1φ.

Fig. 10 Sieving process developed at ESPOL, Guayaquil-Ecuador. (A)Weighing of the total samples. (B) Sieving with a Retsch Sieve Shaker AS 200. (C)Weighing of the different fractions. (D)Stored and labeled samples.

The principal statistical parameters of the grain size distributions were calculated according to Folk & Ward 1957 using the free software Kware SFT (Wohletz et al., 1989): median diameter (Md-phi), graphic standard deviation (Sigma-Phi), graphic skewness (SkG), graphic mean (Mz), inclusive graphic standard deviation (Sigma-I), phi quartile deviation (QD- φ), inclusive graphic skewness (SkI), phi quartile skewness (Skq- φ) and graphic kurtosis (KG).

4.3 Components analysis

The components analysis for particle size between -4φ to -1φ was carried out on a stereomicroscope Olympus SZX 16 with 1X and 0.5X lenses by visual examination and for particle size between 0φ to 3φ using the software JMicroVision (Roduit, 2007). The fraction from 0φ to 3φ was glued on millimetric paper (4.5 x 4.5 cm) and photographed. Subsequently, the picture was uploaded in JMicroVision in which using point counting tool 3 classes have been differentiated: juveniles, lithics, and crystal, as Figure 11 illustrates. During the manual counting, each grain was identified and classified in its class. Some rock fragments present two components; the dominant component was taken into account.

The coarse fractions were studied using optical analysis. For the analysis of the components between -4φ to 1φ, a representative sample was visually examined. The component was classified in 3 components juveniles, lithics, and crystals and later weighted. The representative sample has been taken with the quarter cut-up method that divides a complete sample into four equal parts. Then two of the four-part are removed, and the two remaining parts are joined together to start the process again until a smaller and representative sample remains. This methodology is illustrated in Figure 12.

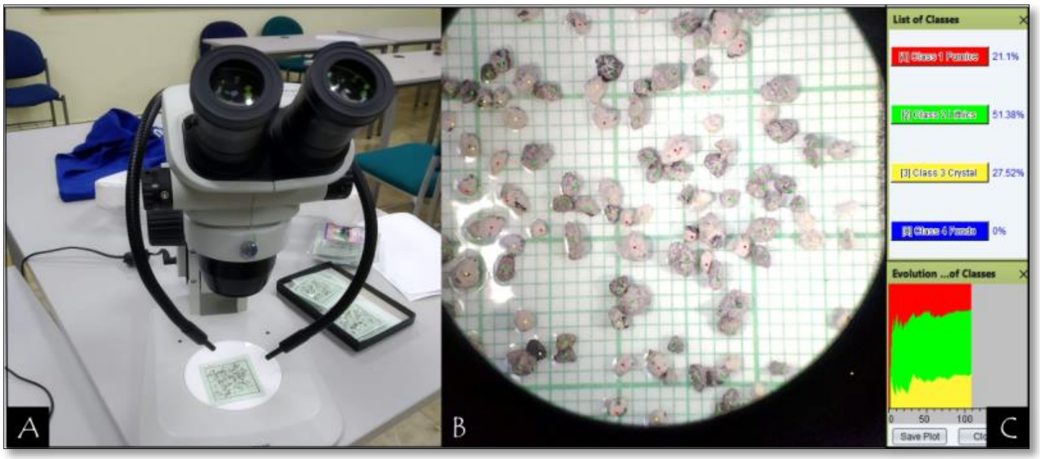

Fig. 11 Components analysis of fine fraction between 0φ to 3φ. (A) Sample glued on millimetric paper in the stereoscopy stage plate. (B)Components in the analyzed sample, little points inside each clast can be distinguished. C) evolution chart (right lower corner) with more tha 100 points, also a table with percentages of the classes (upper corner right): pumice in red, lithics in green, crystals in yellow and background in blue.

Fig. 12. Quarter cut up methodology. (A) Complete sample in a clean surface. (B)Cutting up in equal quartiles. (C) Opposite quartiles has been discarded and the other 2 remaining could be used to count the component fraction. (D) Weighing of the fractions.

Chapter 5: Results

5.1 Stratigraphic Relationships and Facies Analysis

In this work, ten stratigraphic sections were logged in detail. The localization of the stratigraphic sections shown in Figure 13. The studied outcrops are limited by Cuicocha road at the south and Rumihuasi ravine to the north, both highlighted in yellow lines in Figure 13. The stratigraphic sections are named in Romans numbers from I to X, the maximum thickness is 35m, and are distributed in an area of 0,75 km^2. Each outcrop is related to one stratigraphic column, as presented in Figure 14. The columns in Figure 14 are organized from the south to the north to achieve a better understanding of stratigraphy in the area. The

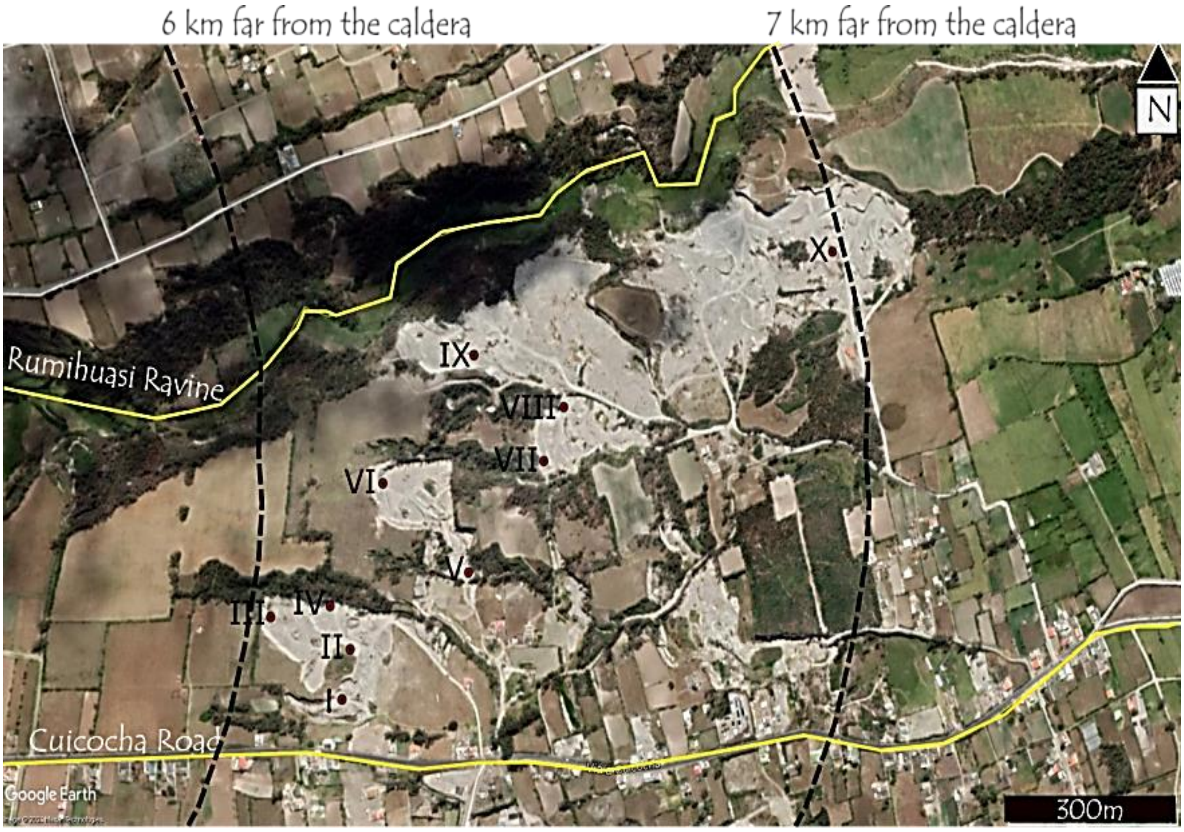

Fig. 13. Map view and distribution of the outcrop for this study. The yellow lines represent Cuicocha road at the south and Rumihuasi ravine at the north which limits our study area.

stratigraphic succession of the studied Cuicocha deposits have been divided into three main units which have been can be identified by letters A (pink unit in Figure 14), B (yellow unit in Figure 14), and C (blue unit in Figure 14) from the bottom of the stratigraphic column to the top. The stratigraphic contacts between A - B and B – C can be described mostly as sharp and well defined. One erosive contact was found between Unit A and B is in column II. No contact

B – C was observed because Unit C was entirely eroded in column VIII. Finally, transitional contacts were observed in unit B between the upper and lower limits in the clast supported breccia in columns II, VII, and VIII.

Fig. 14 Stratigraphic columns and correlations in the studied area. The columns from I to X corresponds to the

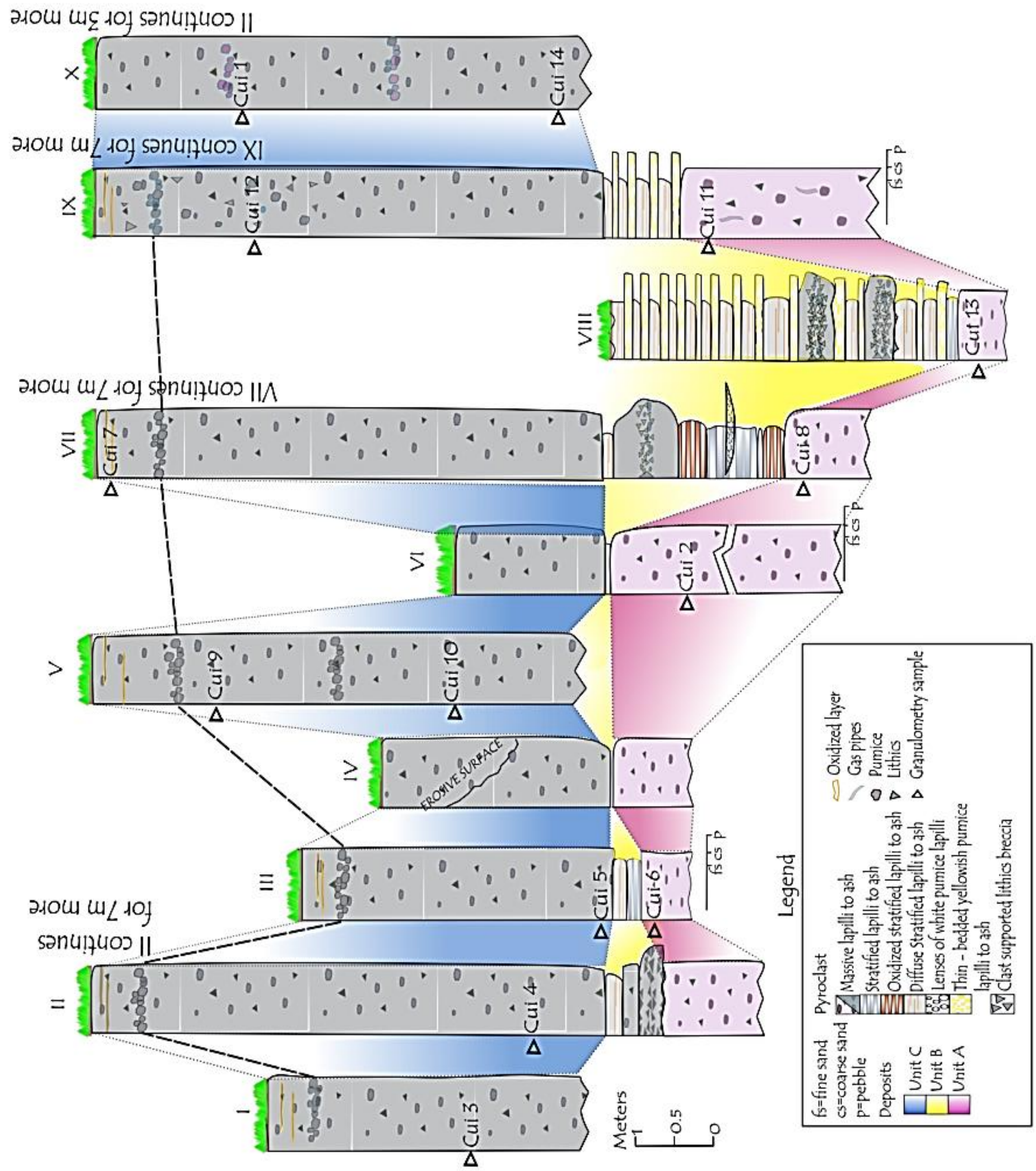

red points from south to north in fig. 13.

Each unit is composed of one or multiple facies. Table 1 summarizes the lithofacies in the study area.

Table 1 Summary of facies

Origin	Aspect	Lithofacies	Description
Primary volcanoclastic deposits	massive	mLA Massive lapilli to ash	Massive fine - coarse ash and fine - coarse lapilli matrix. Matrix supported with blocks of pumice and lithics (size between 3 to 6 cm). Poorly sorted.
		lpLA Lens pumice lapilli to ash	white lens of pumice very poor sorted and with a normal graded sedimentation in an ash groundmass.
		cslBr Class supported lithic breccia	Clast supported monolithic gravel. Lithics fragments between 0.5 to 8 cm. Poor in pumice. Bad sorting and sub-angular to angular clast.
		byLA Thin bedded yellowish Lapilli to Ash	The facies has yellowish pumice of lapilli and block size well to moderate sorted. Rare (or absent) lithics could be found.
Secondary deposits	stratified	dsLA Diffuse stratified lapilli to ash	sub-parallel stratification of millimetric size. Fine to coarse ash layers
		odsLA Oxidized diffuse stratified lapilli to ash	sub-parallel stratification of millimetric size. Fine to coarse ash layers with yellowish color because oxidation

The textural features, general aspect, geometrical relationships, and abundance of components in a stratum define the facies. The main feature to classify the facies here is related to the presence or absence of stratification. If a volume of rocks has one single texture with the same type of matrix and clastic components, then this volume of rocks has a massive facies. On the other hand, if a unit displays layering or stratification, then this is a (diffuse) stratified facies. The stratigraphy in this study is limited to six lithofacies; four of them are massive, and two stratified. The lithofacies are labeled following the lithofacies description developed by Branney & Kokelaar, (2002), which do not take into account the origin of the unit and is wholly related to the observed lithological characteristics.

Unit A presents thicknesses that vary from 0.5m to 4 m, as can be seen in columns II, III, IV, VII, VIII, and IX. The base of the Unit does not outcrop in the study area. Unit A is characterized by poorly sorting, matrix-supported rock fragment of pumice and lithics, lenses of clast supported pumices which are visible in columns II, III, V, VII, and IV, and rarely clast supported breccia lenses. The pumices in this unit are sub-rounded, and the lithics are sub-angular both in sizes from lapilli to blocks. The clasts are randomly distributed in the groundmass, and no fabric-related features (i.e., lineation and imbrication) were identified neither in the clasts nor in the matrix. The matrix is made of lapilli to ash size fragments of pumice, crystals, and lithics. Additionally, one remarkable feature is the pinkish color in this unit that makes it distinguishable from Unit 3 that has a similar texture as it is shown in figure 15.

Unit B is a sequence of layers characterized by intercalation between diffuse stratified and oxidized diffuse stratified facies and no stratified layers of variable thickness. For example, the variation in thickness can be seen by comparing Figures 15b and 16. The sequence of facies and the intercalated layers in both figures are different. Figure 15b is made of one single diffuse stratified facies. (dsLA); meanwhile, in Figure 16, several diffuse stratified facies (dsLA) are intercalated with beds of yellow pumice (byLA). Unit B appeared in every column except I and X with variable thickness from 1cm to 4m. Occasionally, clast supported lithic breccia (cslBr) were found, as can be seen in Figure 16 and also lens pumice lapilli to ash (lpLA).

dsLA, and odsLA show millimetric parallel to sub-parallel stratification of very fine to medium ash with good sorting, which thickness varies from 0.01 m to 0.60m. The facies rarely contains lithics and pumice fragments immersed in the ash groundmass, and some layers present normal and inverse grading with mostly transitional contact between dsLA and odsLA. All the described features could be appreciated in the photograph of Figure 16. Furthermore, byLA is made of yellowish pumice of pebble size, with well to moderate sorting. The yellowish pumice forms diffused stratified layering lapilli to ash, and parallel contacts clearly separate the beds. The pumices are immersed in a matrix of fine ash, in which the lithics are rare (or absent). No lineation nor imbrication was found in the clasts. Finally, Figures 16 - 17 shows byLA intercalated with other stratified units of dsLA and lpLA in the thickest section (4m) of Unit B represented by column VIII.

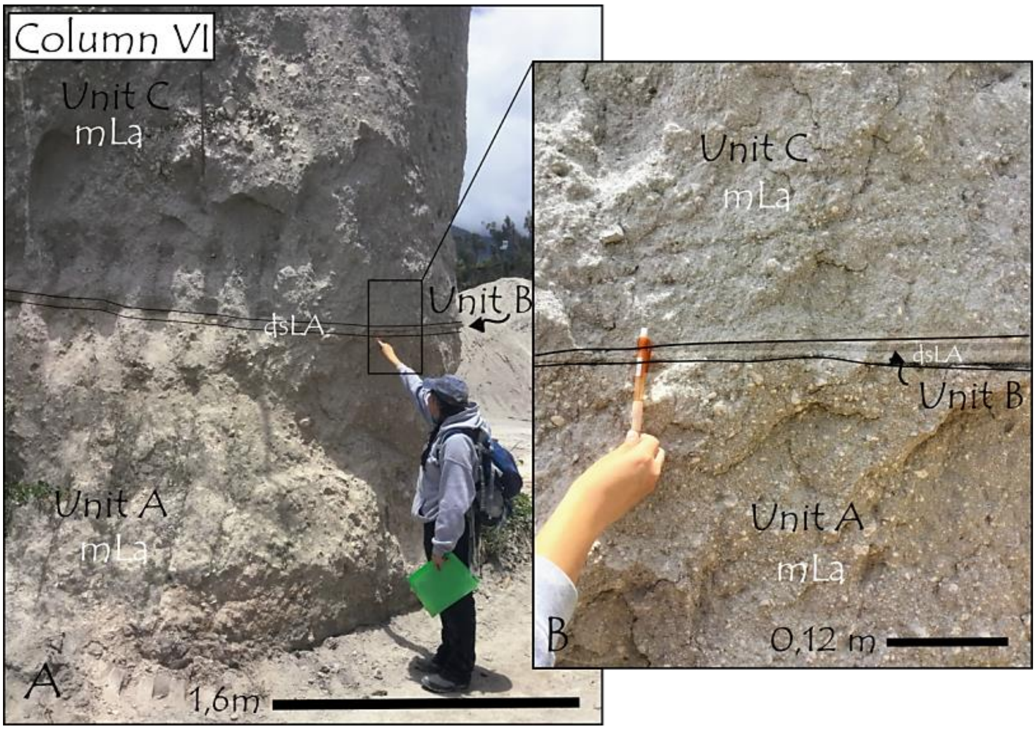

Fig. 15 The outcrop corresponds to column VI. a) Unit A is at the bottom, looks slightly pinkish and massive, and b) show the texture in detail with clast randomly distributed in the matrix. The three main units A, B and C and its facies are label.

Fig. 16 Unit B variability of facies in 4m thickness outcrop that corresponds to column VIII.

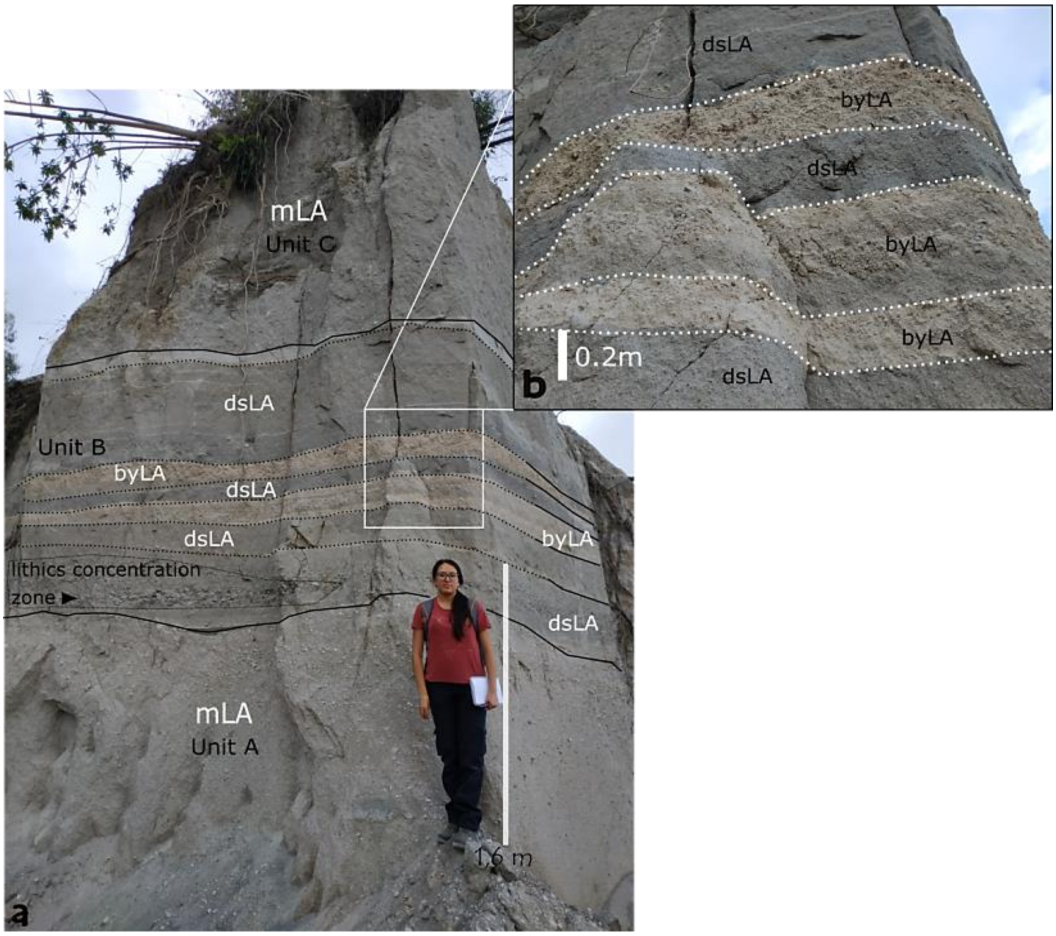

Fig. 16 Thin-bedded yellow pumice lapilli (byLA) intercalated with other stratified units of sLA, and dsLA in the most thicker section (4m) of Unit B represented by column VIII.

The less typical facies in unit B are lpLA and cslBr, and each one just appears once in all the study area. lpLA white pumice wedge has a thickness of 0.01 cm to 0.15 m and 6m long. This wedge was in the middle of unit B at the section represented by column VII in Figure 18. It is very poorly sorted, and the pumice forms a normally graded pattern from medium lapilli to pebbles in an ash matrix. In general, no lithics fragments were found, and fine black material covers various pumices.

Likewise, cslBr facies is formed by beds from 0.2 to 0.5m thick. The facies is poorly sorted and ash-rich layer that consists of sub-angular to angular imbricate grey lithic fragments in block size in an ash-lapilli matrix. The clasts show no alteration and are organized in a gradational fining upward pattern. Some clasts are covered by a black film of fine size material. Finally, a few well-sorted round pumice in lapilli size is enveloped in the groundmass of cslBr. All the described features are illustrated in Figure 19.

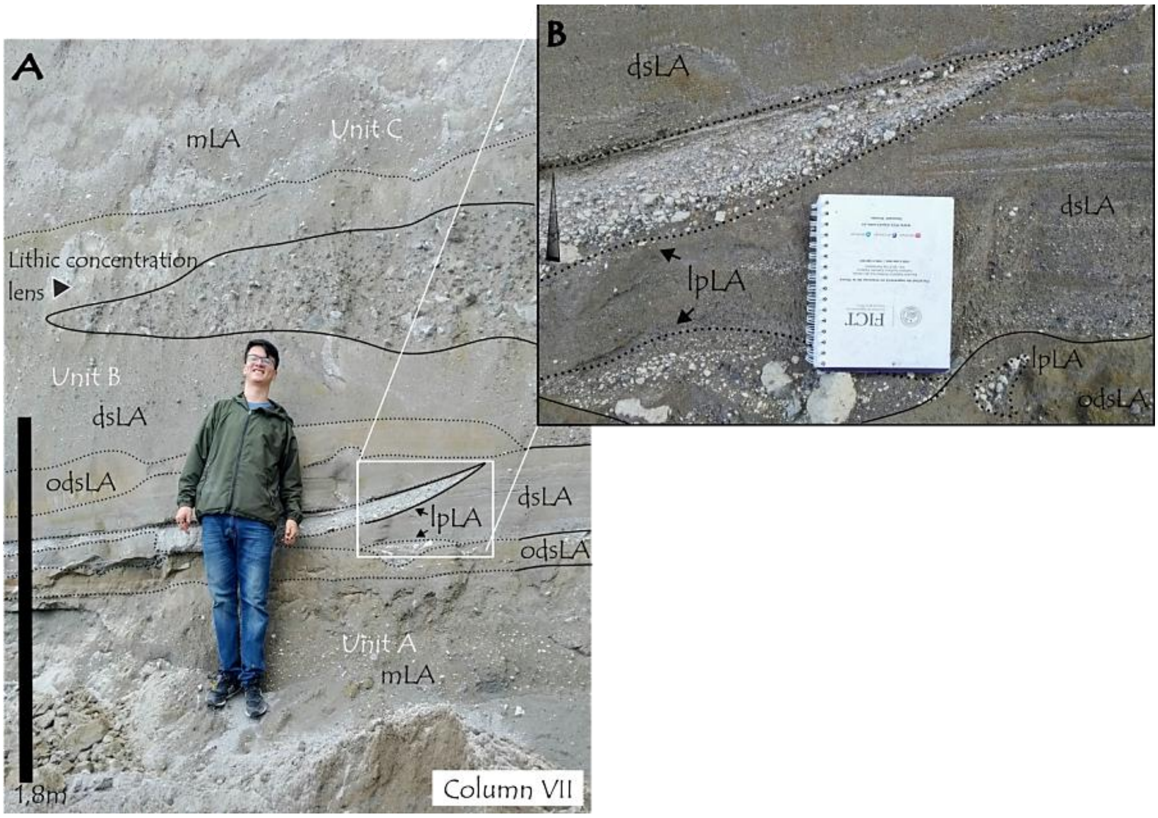

Fig. 17 Pumice lenses. The photographic the left side shows the location of a lens of pumice and the photograph to the left. Show in detail the texture and geometry of the lens.

Finally, Unit C is the thickest found in the study area and varies from 2m and 15m-thickness as represented by Figure 20a-b. This unit is characterized by the lithofacies mLA similar to Unit A. The principal difference between both is a grey color in unit C that and well-defined levels of well-sorted pumice as represented in columns I, II, III, V, VII, IX, and X. The pumice clasts have 3cm to 5cm size and are sub-rounded. In the last 50cm of unit C, various features can be observed, such as thin slightly orange layers due to oxidation (Fig.20c), and 10 to 20cm of material that is being converted into soil. Finally, the grass covers all the sequences.

Due to limitations in figure size, we cannot show the total extension of unit C in columns II, VII, and IX that achieve 15m thickness each one. Because of that, the columns expose a break in the middle. In some outcrops like those at the southern and northern limits of the study area, only unit C outcrops, as represented in columns I and X, respectively. The same happens in column V, which is located in the middle of the studied area. None of these columns expose the bottom limit of unit C. Moreover, the unconsolidated material of unit C has been completely removed from column VIII, and partially eroded from column IV that has marked erosional contact in the middle of the deposit. Meanwhile, column VII lacks unit C suggesting an erosional process that removed the material to another side.

Fig. 18 Lithic breccia as transitional boundary at the lower limit of the stratified Unit. The unit is 50 cm in thickness, with a fining upward gradation.

Fig. 19 Unit C presents a variable thickness. Unit C in (a) has been partially removed, an erosional surface was found. The photography corresponds to column IV. Meanwhile (b) has a 12m of extension and is represented by column I. Commonly, the upper part of Unit C develops oxidized zones (c) and an andisol (b).

5.2 Other features

Gas Pipes

Gas pipes could be identified because of their blackish color fine material that covers the surrounding rocks. Figure 21 details photographs of texture and extension of rectangular gas pipes can be seen in column VIII (Fig. 16) in the boundary between Unit A and B. Other gas pipes are more extended in length 0.03-0.05m and have 0.02-0.03m thickness. Furthermore, elongated gas pipes were found in the section represented by column IX in Figure 22. These gas pipes are inside Unit A, and they have 0.2 to 0.3m in length and 0.02m of thickness.

Faults

Fig. 20 Gas pipes detail.. A) corresponds to the detail of gas pipes in column VIII in a byLA facie, finger as scale B) Gas pipes detail in the contact between odsLA and dsLA in column VII, the pencil tip is 1cm length.

Faults in the deposit are scares. Figure 22 shows the only faulted section, which is restricted to 2m in thickness and 6m in length. This section exposes a graben and horst structures inside Unit B. The low-standing fault block at the right side in the photograph is the graben and is bounded by opposing normal faults (look at the arrows in Fig.21). Towards the left of the graben in the middle of the picture, there is a high-standing block called horsts limited by opposing normal faults. The other faulting surfaces are parallel to those that limit the graben and the horse (Giles, 1968).

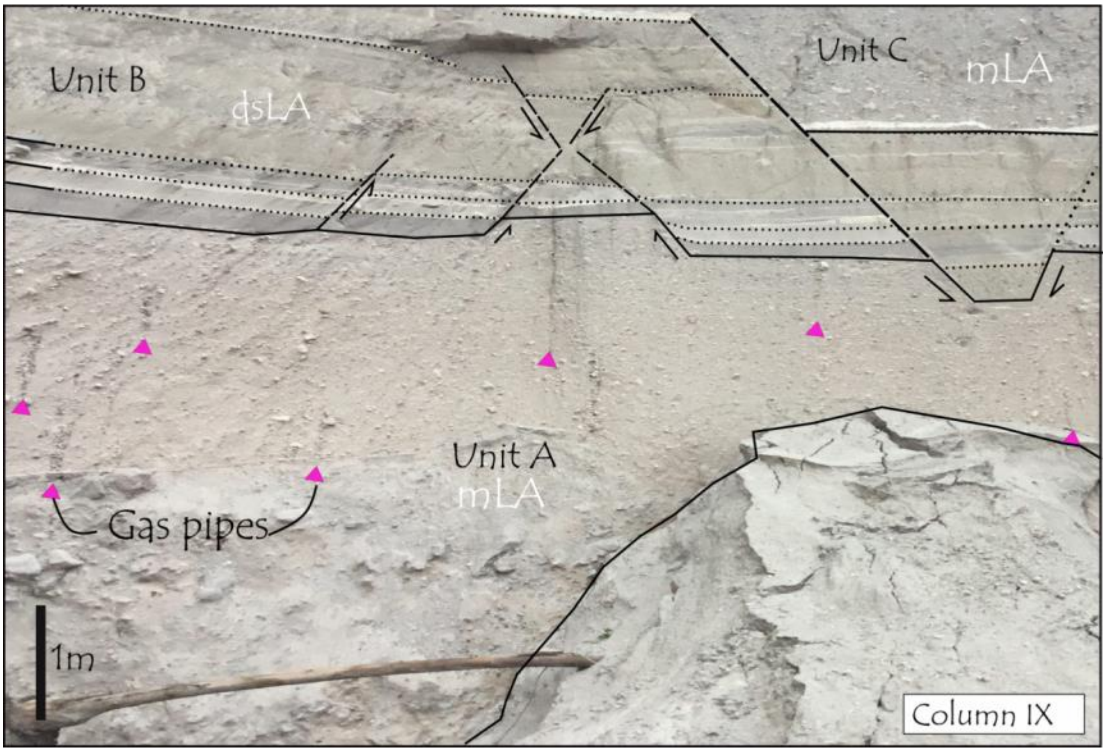

Fig. 21 Gas pipes in a deposit represented by column IX. The gas pipes can be differentiated based in the typical blackish color that cover the rocks in the surroundings. The pink triangle points the base of the pipes that are extended in unit A.

5.3 Grain Size Distribution and PDC Components

PDC's are made of volcanic material of variable size and shape released in an eruption. Following the results are presented in histograms that show grain size distribution in phi intervals. The grain size distribution quantifies the percentage of each particle in the sample at different levels in the stratigraphy of Unit A and C. In general, both units A and C show similar trends along with the thickness. Unit B was not sampled because this work is focused on the two premier events represented by concentrated PDC and not in the dilute PDC.

Fourteen histograms were constructing based on the granulometry information of a total of 14 samples (Cui 1 - Cui 14). The histograms in Figures 23 and 24 show the size-frequency distribution for each fraction of the phi size from -4φ to 11φ and are shown divided by depositional units. In this way, Figure 23 represents four samples taken at Unit A, while Figure 24 represents the samples from unit C.

Based on the histograms, particles between 2φ and 3φ are the most abundant as reflected by the peak in the histograms. Most of the samples have their statistical mode (i.e., the peak of the curve) at 2φ size fraction. Moreover, few samples have a significant high fraction of coarse material. Cui 1, Cui 9 in unit C and Cui 2 in unit A have a secondary peak at -4φ, while Cui 3 at -2φ. Moreover, there is a decrease in the number of particles in the fraction 5φ to 11φ (silty clay fraction). In general, deposits do not show an important variation in the granulometry, units, or in the horizontal and vertical distribution of samples. The dominance of sand size material can be seen in Figure 25, which shows a ternary diagram of sand, gravel, and fines. Finally, the percentage per fraction of gravel, sand, silt, and clay are summarized in Table 2.

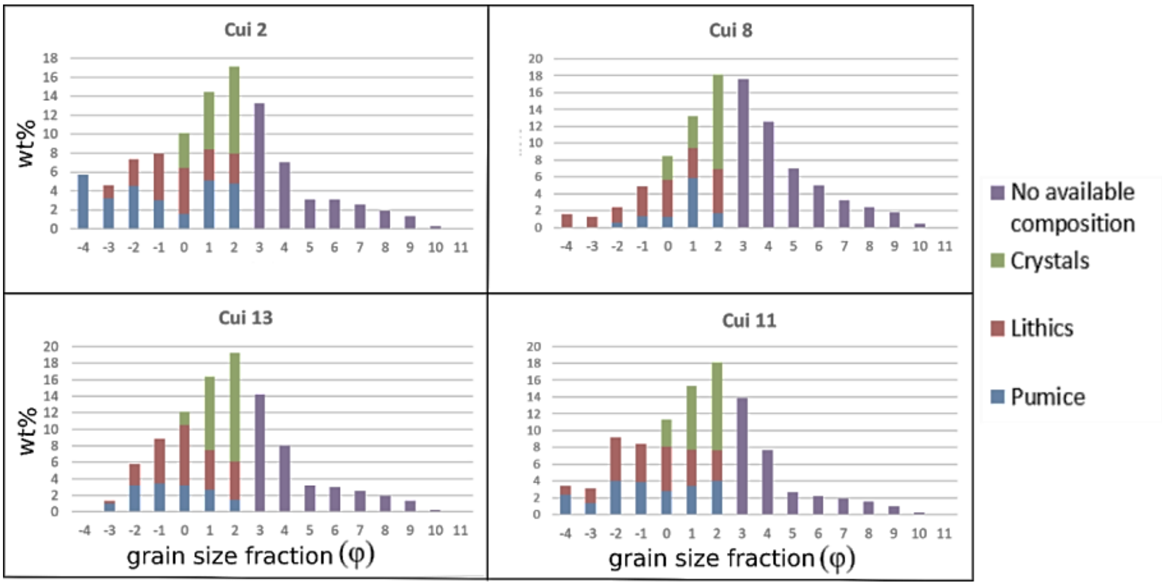

Fig. 22 Unit A histogram of the distribution of φ grain size fraction vs. % weight per each one of four samples from. The fraction from -4φ to 2φ includes the distribution of the components of each φ fraction.

The estimation of the volume percent of pumice, lithic clasts, and crystals in each fraction and the description of the textural characteristics in individual clast was carried out for the 14 analyzed samples. Juvenile rock, those that have been created during the eruption, is the first component. They can be partially crystallized or no crystalized, for example, pumice and glass, respectively, because of the rapid quenching and chill of the material. These particles are characterized by a degree of vesiculation as a consequence of the existence of volatiles in the magma and their ex-solution (Cas & Wright, 2012).

Pumice clasts were found in all the analyzed fractions. It is present in size from blocks to fine ash, and show a typical milky white to a slightly grey color. The juvenile material contains black euhedral prismatic crystals of hornblende and some show perfect cleavage planes. They could be easily identified in geometrical shapes similar to black lines or black dots. In hand samples (block size), also crystals of amphibole, plagioclase, and opaque have been found. Just a few expose visible porosity in lapilli size and elongated vesicles. No glass has been found.

Pumice could have an equal distribution as samples Cui 11, Cui 12, and Cui 14 or a bimodal distribution usually with two peaks the first between -2φ or -4φ size fraction and the second in 2φ size fraction like the rest. The pumice clasts have crystals of plagioclase, pyroxene, and quartz visible with hand lenses, all of them are anhedral to subhedral, and the size is less than 2 mm.

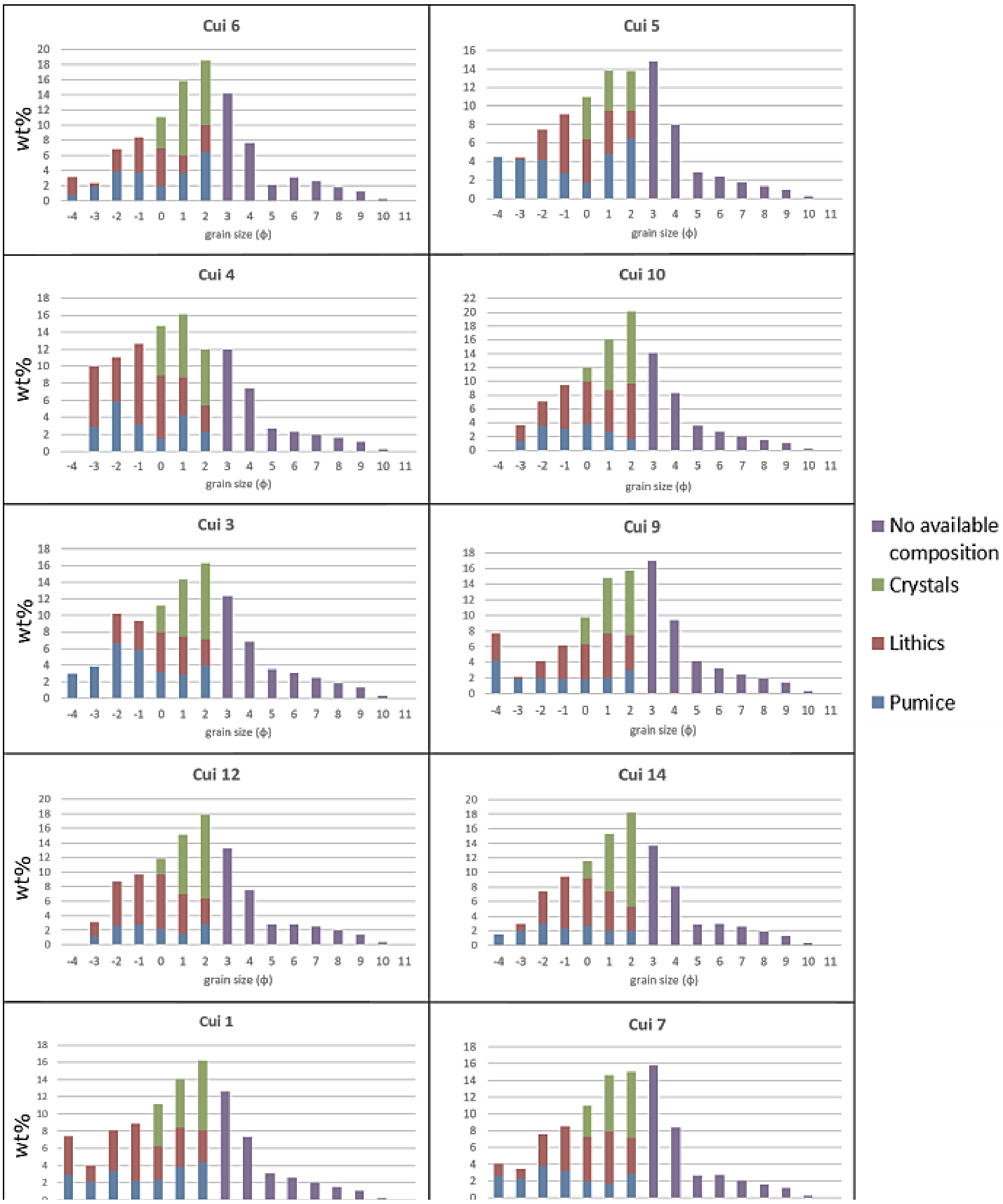

Fig. 23 Histogram of the distribution of φ grain size fraction vs. % weight per each one of the 10 samples from Unit C. The fraction from -4φ to 2φ includes the components fraction of each φ fraction.

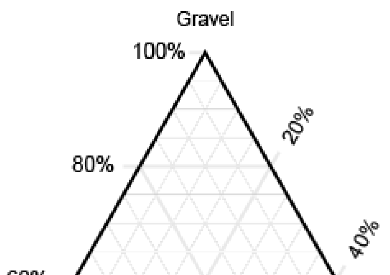

Table 2 Particle size from the ignimbrite samples from Cuicocha.

Unit	Samples	Gravel (-4φ to -2φ)	Sand (-1φ to 4φ)	Silt (5φ to 8φ)	Clay (≥9φ)	Fine (St+Cl)	Matrix (-1φ to 11φ)
Unit A	Cui 7	15.05	73.22	8.95	1.42	10.37	83.59
	Cui 1	19.41	70.12	9.1	1.22	10.32	80.44
	Cui 4	16.17	73.87	8.57	1.36	9.93	83.8
	Cui 12	12.96	75.13	10.06	1.63	11.69	86.82
	Cui 9	14.03	72.44	11.62	1.7	13.32	85.76
	Cui 3	17.01	70.24	10.97	1.56	12.53	82.77
	Cui 10	10.63	81.64	9.65	1.26	10.91	92.55
	Cui 14	11.81	76.25	10.17	1.65	11.82	88.07
	Cui 5	16.31	70.32	8.2	1.19	9.39	79.71
	Cui 6	12.27	75.56	9.56	1.48	11.04	86.6
	Average	14.57	73.88	9.69	1.45	11.13	85.01
Unit C	Cui 11	15.72	74.42	8.27	2.5	10.77	85.19
	Cui 13	7.09	78.79	10.7	1.6	12.3	91.09
	Cui 8	5.19	74.72	17.6	2.21	19.81	94.53
	Cui 2	17.72	69.77	10.65	1.61	12.26	82.03
	Average	11.43	74.43	11.81	1.98	13.79	88.21

Lithic fragments are the denser components in a PDC. The lithic fragments are divided into three categories depending on their origin. Non- vesiculated lithic fragments from magma are cognate lithics, but if it was ejected from the country-rock during the explosion (i.e from the volcanic vent), it is an accessory lithic, and if the fragment was picked up by the current is an accidental fragment (Cas & Wright, 2012). They can be differentiated based on the texture, color, and sometimes oxidation on the surface.

Some lithics are characterized by gray color and a component of plagioclase with vitreous/glassy luster, and the pieces are covered with a very fine grain of milky white matrix. Other lithics have a dark grey to a black color and an aphanitic texture. Additionally, some samples of this texture present a yellow and orange color because of oxidation. Most of them are sub-angular and angular; some are greenish clast and other slightly reddish and mostly smaller than the pumice. The lithics correspond to dacite-andesite from Cuicocha dome explosion and greenish andesites from Macuchi Fm,. (von Hillebrandt, 1989). The microcrystals correspond to prismatic hornblende and amorphous plagioclase. The percentage of lithics in the fraction $<2\varphi$ is mostly present in the same proportion in each particle size, this could be evidence more clearly on Cui 1, Cui 4, and Cui 9.

Porphyritic magmas form crystals, and those are fractured during explosive eruptions and can be found as part of juvenile fragments (Cas & Wright, 2012). The crystals can be transparent, slightly white, or black. The transparent and white are mostly anhedral transparent with a vitreous luster; because of that, they are plagioclase. Meanwhile, the black ones are pieces of euhedral to subhedral prismatic crystals of hornblende. In the histograms, the crystals increase in fraction toward the fine fraction.

Figure 26 corresponds to 2 φ size fraction of sample Cui 5 and showing the different components that are labeled. This is the common component that were found in all the samples and has previously been described. The average percentages of components in each sample could be sawed in the ternary diagram in Figure 27, where is clear that the samples mostly content crystal or crystal fragments and all the sample remain around 20% of lithics, and juveniles vary between 35% to 75%. The samples from unit A are pink, and the samples in unit C are blue.

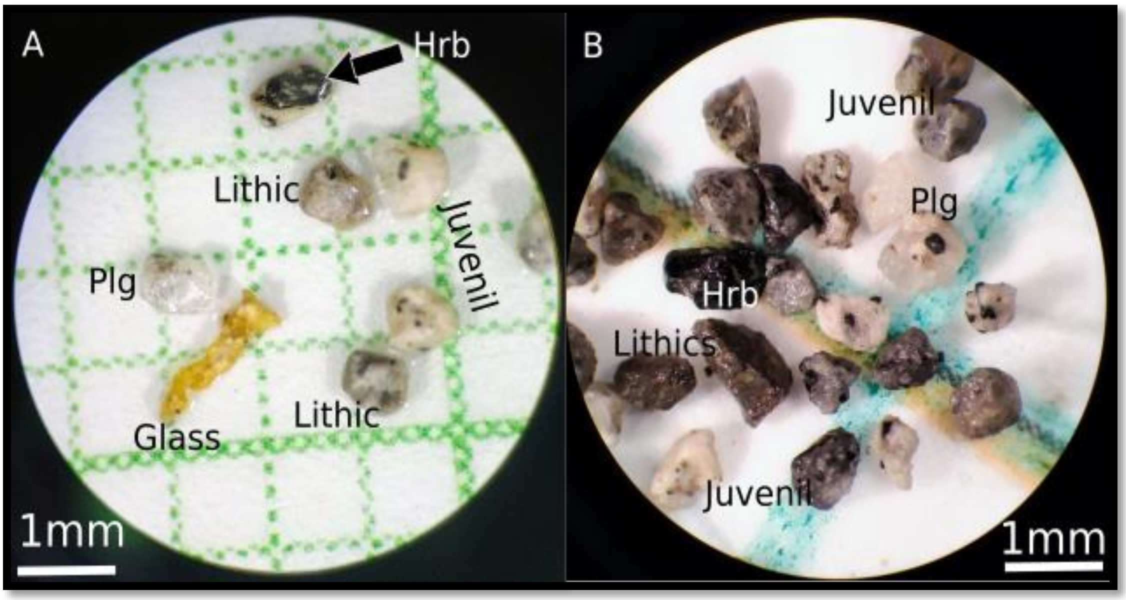

Fig. 25 Detail photographs of the components of the pyroclastic current from Cuicocha. The milky white corresponds to juvenile fragments. Vitreous dark crystal of hornblende incrusts in a juvenile, and the translucent crystals corresponds to plagioclase. The lithics have grey color with hornblende intrusions. In A) there is a yellowish very angular glass fragment, which was the only one found among the analysis of components.

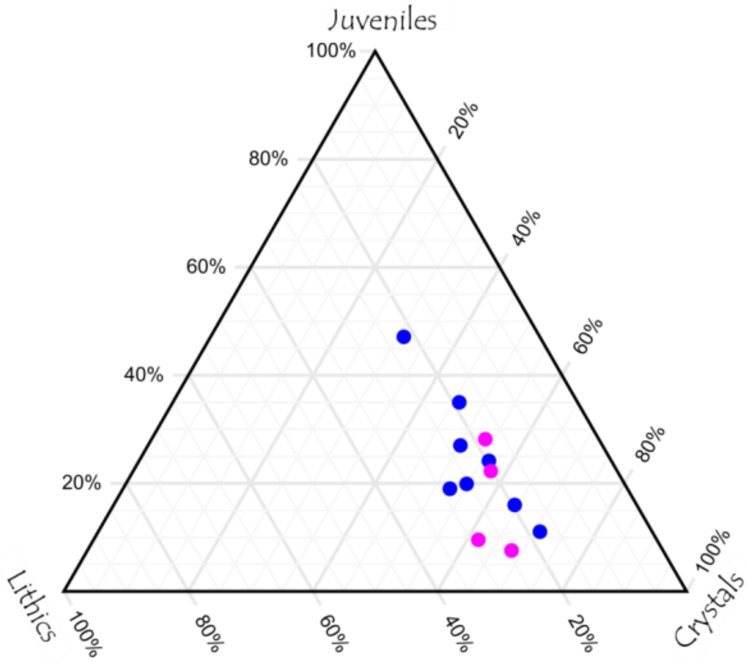

Fig. 26 Ternary plot about the composition of the 14 samples from PDC in Cuicocha.

The statistical analysis of this distribution and the histograms provides information to characterize the type of flow. Besides to understand the complete size characteristic of the deposit, Inman (1952) recommends using four statistical parameters, and these are mean grain size, standard deviations, kurtosis and skewness, which can be obtained from the distribution in the histograms (Inman, 1952; Folk & Ward 1957; and therein). Below is a summary of the meaning of each statistical parameter and how to obtain each one.

The median size (Md) is a central tendency measure. It s calculated as φ16 which is the median or average size of the coarse third of the sample (-4φ to 2φ), φ84 is the median or average size of the finest third of the sample and φ50 is the average of the middle third (Folk & Ward, 1957). The formula determines Md:

$$Md = \frac{\varphi 16 + \varphi 50 + \varphi 84}{3}$$

Standard deviation is associated with sorting (σ) and represents a measurement of the grade to which each assembly of numbers is different from the average. In this way, the sorting evaluates the sorting of a sample of rocks. The formula founds standard deviation:

$$\sigma = \frac{\varphi 84 - \varphi 16}{4} + \frac{\varphi 95 - \varphi 5}{6.6}$$

Sorting values have the following equivalency: $\sigma < 0.35$ = very well sorted, $\sigma > 0.35$ and < 0.50 = well sorted, σ >.0.50 and < 1.00 = moderate sorted, $\sigma > 1.00$ and < 2.00 = poorly sorted, $\sigma > 2.00$ and < 4.00 very poorly sorted, and $\sigma > 4.00$ = extremely poorly sorted.

Skewness (Sk) determines the asymmetry of the central part of the distribution. An Sk equals 0.00 represents a perfect symmetrical curve like a Gaussian distribution. Negative values correspond to a tail in the coarse fraction, while the positive is a tail in the fine fraction; the limits in the measure are -1 and +1, respectively (Folk & Ward, 1957).

$$\mathrm{Sk} = \frac{\varphi 16 + \varphi 84 - 2\varphi 50}{2(\varphi 84 - \varphi 16)} + \frac{\varphi 5 + \varphi 95 - 2\varphi 50}{2(\varphi 95 - \varphi 5)}$$

Skewness values have the following equivalency: Sk >-1.00 and < -0.30 = very negative skewed, Sk >-0.30 and < -0.10 = negative skewed, Sk > -0.10 and <+0.1 = nearly symmetrical, Sk > +0.10 and < +0.30 = positive skewed, and Sk >+0.30 and < +1.00 = very positive skewed.

Kurtosis (K_G) is a measure of the sharpness of the peak of a frequency-distribution and the concentration of results in the tail of the curve. The KG values have the following equivalency: $K_G = 1.00$ is related to the geometry of a normal curve, $K_G < 0.67$ = very platykurtic, between

0.67 – 0.90 = platykurtic, K_G between 0.90-1.11 = mesokurtic, K_G between 1.11-1.50 = leptokurtic, K_G between 1.50-3.00 = very leptokurtic, and K_G > 3.00 extremely leptokurtic. K_G is evaluated through the elongation of the curve (Inman, 1952), and it is measured with the following formula:

$$K_G = \frac{\varphi 95 - \varphi 5}{2.44(\varphi 75 - \varphi 25)}$$

Table 2 shows statistical parameters from grain size distribution, obtained from the size fraction distribution of all samples in this study. The table separated the samples from units A and C. On the one hand, Unit A has the following results: the Md values fall between 0.65 φ to 2.02 φ (average value is equal 1.13φ). In his way, the data reflects the dominance of the sand size particles (-1φ to +4φ). Moreover, the value σ in the samples is positive and in a range of 2.47 to 3.01 (the average value is equal to 2.68), which suggests a poorly sorted deposit. The Sk range between -0.23 and 0.02 that reflect a tendency of fragmentation dominated by the production of sand-size particles. Finally, the KG is in a range of 1.14 to 1.24, which corresponds to a leptokurtic tendency.

Besides, the result in unit C is: Md have values between 0.45 φ to 1.05 φ (average value is equal to 0.77φ), which implicates a dominance of sand-size particles (-1φ to +4φ). The value σ in the samples is positive and in a range of 2.27 to 2.97 (average value is equal to 2.71), which advocates poorly sorted deposits. The Sk ranges between -0.25 and -0.12 (average value is equal to -0.16). Finally, the KG is in a range of 1.06 to 1.32, which corresponds to a mesokurtic to leptokurtic tendency. The data of the statistical parameter is summarized in Table 3.

The cumulative curves, in Figure 28, show important changes in slope, and a similar trend between the samples. In order to effectively compare our fourteen samples, I took two samples of well study pyroclastic flows in Mount (Mt.) Saint Helens from 1980 eruption (Fig. 28) (Kuntz, et all., 1982). Mt Saint Helens samples correspond to 0% and 20% weight percentage of coarser material, and the samples in this study start in between the range established by the samples of Mt Saint Helens. All the samples follow similar trends after -1φ. All samples tend to increase from lapilli to coarse ash content with a steep slope. After the coarse ash, the finer particle distribution has a shallower slope with the tendency to become horizontal. Meanwhile, the tendency in the samples in this study becomes almost flat after 5φ, the samples in Mt. Saint Helens accumulates all the finer material of 5φ grain size or minor in the 5φ.

Table 3 Statistical parameters from grain size distribution the ignimbrite samples from Cuicocha.

Unit	Samples	Median phi size (Md)	Standard Deviation (σ)	Skewness (Sk)	Kurtosis (K_G)
Unit A	Cui 7	0.73	2.8	-0.15	1.15
	Cui 1	0.45	2.96	-0.25	1.1
	Cui 4	0.55	2.69	-0.13	1.06
	Cui 12	0.85	2.7	-0.13	1.15
	Cui 9	1.05	2.97	-0.18	1.32
	Cui 3	0.68	2.87	-0.18	1.1
	Cui 10	0.98	2.47	-0.15	1.18
	Cui 14	0.93	2.65	-0.13	1.17
	Cui 5	0.58	2.81	-0.15	1.07
	Cui 6	0.9	2.27	-0.12	1.25
	Average	0.77	2.71	-0.16	1.16
Unit C	Cui 2	0.65	3.01	-0.23	1.18
	Cui 8	2.02	2.56	0.02	1.21
	Cui 13	1.18	2.47	-0.05	1.24
	Cui 11	0.67	2.68	-0.23	1.14
	Average	1.13	2.68	-0.12	1.19

A plot of the standard deviation versus median grain size is useful to compare deposits of a different mode of origin and types of PDC. Every sample start between 0% and 10% of concentration on the coarse lapilli fragments, gradually the curve grows accumulating between 10% to 30% of the material in the lapilli size. Then the curve grows with the steeper slope until it accumulates 80% to 90% of the fragments in the coarse ash fraction. Finally, the curve tends to become flat for the fine ash particle size.

Figure 29 illustrates the sorting change along with the different grain sizes. The diagram includes the countors for pyroclastic flow (Fl) and pyroclastic fall (Pa) proposed by Folk & Ward (1957). The fourteen samples in this study are plotted over Fl field. The bad sorting for all the sand size measures, which is a classical finding for ignimbrites that come from concentrated PDC (Folk & Ward, 1957).

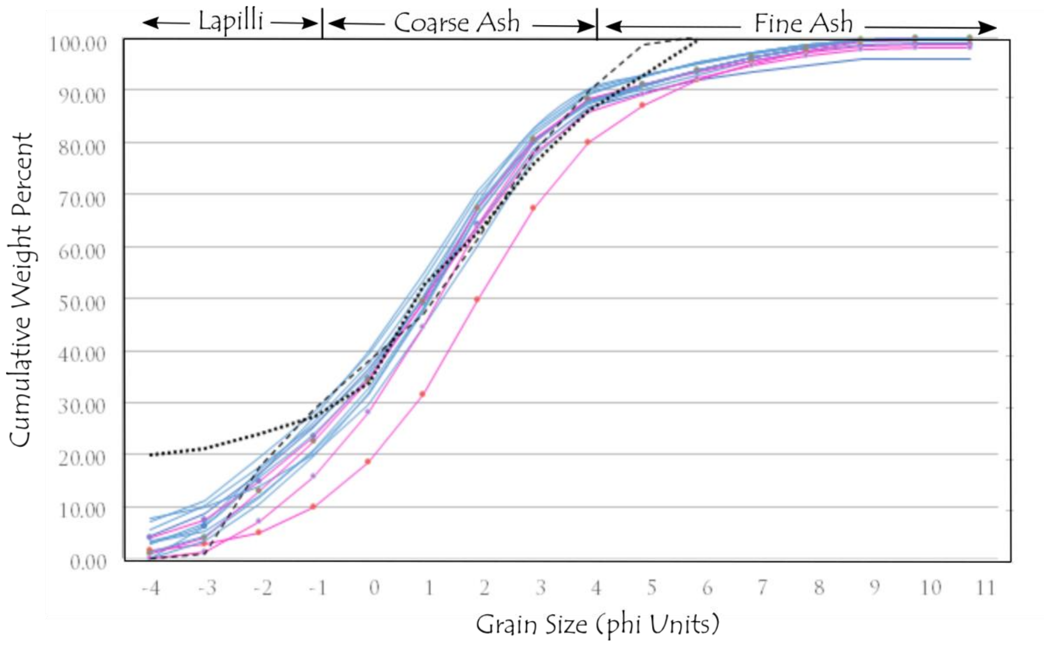

Fig. 27 Cumulative curves for Cui 1 – Cui 14 in pink (Unit A), blue (Unit C) and black for Mt. Saint Helens. The samples show an equal distribution of size in the sample. Both Saint Helens samples and samples in this study follow similar trends.

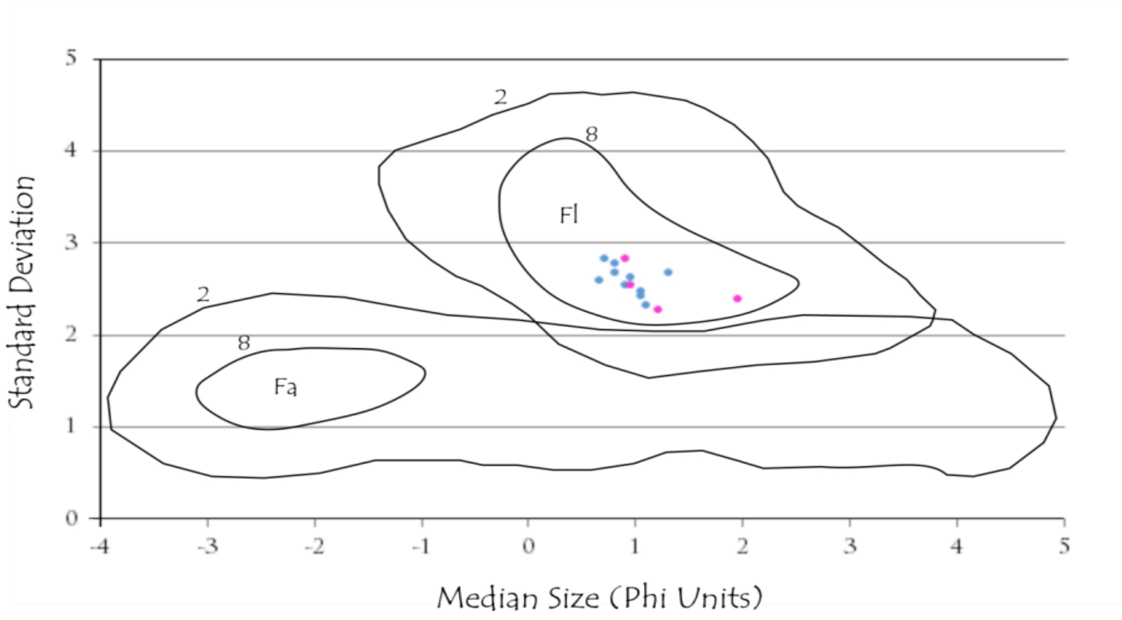

Fig. 28 Scatter plot of mean size vs. standard deviation. The circles represent the set of samples. Samples in unit A are represented with pink and samples from Unit C are represented in blue.

Chapter 6: Discussion

6.1 Stratigraphy

Three units A, B, and C conform to the PDC deposit. The three units were established after developing ten stratigraphic sections. Unit A and C correspond predominantly to mLA facies deposits associated with a primary volcanoclastic deposit. Unit B corresponds to a sequence of several diffuse stratified facies, and massive facies with both primary and secondary deposits located in the middle between Unit A and Unit C. None of the deposits are welded, there was no cover vegetation and exposure was excellent. Following the units are interpreted based in the stratigraphic position from bottom to top.

The first unit in the stratigraphic record of Cuicocha is associated with CFE, which destroys the dome and produces the PDC current. This PDC constitutes Unit A, and it is characterized by a massive facie mLA with randomly distributed good sorted pumices and lithic clast with no grading in a pinkish fine ash matrix. Unit A is restricted to the central part of the studied area and is extended toward south and north with thicknesses between 2 - 4 m. The Unit does not outcrop anymore at the borders. According to Bradley and Kokelar (2002), the mLA facie corresponds to the most common among ignimbrites, and its parental current is a concentrate PDC or pyroclastic flow. The bad sorting, massive appearance, and lack of preferred lineation or arrangement in the components is a consequence of steadiness during a sustained deposition of the current. The subrounded pumice and subangular lithic class are associated with little transport from the emission center to the emplacement place. There are minimal changes in the vertical axis in the deposit as a consequence of a constant current been deposited.

The reactivation of the CCVC in Cuicocha emission center produces a second PDC, which base is made by a bedded deposits that progressively evolve to a massive deposit with similar characteristics of unit A. Unit B corresponds to the deposit with the intercalation of different diffuse stratified (dsLA and odsLA) and massive beds (plLA and clBr). This unit has 1cm thickness but can grow until 4m. Some facies like plLA and clBr can come from primary activity in the volcano, while the dsLA and odsLA present sedimentary features as subparallel stratification that allows us to think that it is a secondary deposit due to erosional and weather processes. Therefore, unit B is a deposit of successive surge, and rework deposits piled one on another.

The thickness of the deposit B is probably associated with the paleorelief in the zone. The south slope of Cuicocha is cut by numerous southeast trending ravines because of the hydrographic system in the area. Naturally, more material could be deposited in channeled sites than in the topographical higher reliefs. Even nowadays, the relief consists of elevations and channels that are being eroded, especially by precipitation and anthropogenic factors. Then, it is probable that the volcanic material from Unit B has been deposited preferentially filling the channels, but also less thick layers covered the paleo topography higher. According to Rowley et all. (1982) this type of deposits come from the ash cloud above the basal ground-hugging pyroclastic flow, or from ground surge associated with the pyroclastic flow itself. However, the stratification in dsLA and odsLA, plLA, and clBr are a consequence of progressive deposition during a gap of time in steady and unsteady currents that segregate different material in dependency the mechanism of deposition. This study is not supposed to go deeper into the understanding of this Unit; that is why its analysis finishes here.

Unit C is overlying B, and it is predominant in the studied area. It has a maximum thickness of 15 m, and in some parts, the upper part of the deposit has been eroded because of its low degree of compaction. Randomly distributed pumices and lithic clasts in a fine grey matrix conform to the texture, which does present neither stratification nor alignments in the components. Nevertheless, a continuous pumice level in the upper part of the deposit can be traced in all the areas. Then, observations suggest a large current been transport over all the areas, and the material transported was progressively deposited in steady conditions as a consequence of the turbulence in the flow in similar conditions of those in unit A.

Overlying Unit C, a significant amount of material, has been transformed into the soil. Each centimeter of soil requires at least 50 years (1 inch per 100 years) to be formed. Besides, the oxidized lenses in the upper part in Unit C are evidence of transformation into soil. They are linked to the effect of percolating rainwater that dissolves various components of the ignimbrite as phosphates and catalyzes the weathering of ferromagnesian and feldspathic minerals on sand grains, which corresponds to the first stages in soil formation processes (Natural Resources Conservation Service, n.d).

One unexpected feature in the field is related to the color in mLA facies. Even when the texture and component between units A and C are practical the same, the pinkish color in Unit A suggests a higher temperature high enough to promote the oxidation of hematite at the time of emplacement according to Hillebrandt (1989). According to Ovalle et al. 2018, the collapse of the volcanic edifice or caldera formations stimulates bubble ex-solution and heterogeneous nucleation on magnetite and Fe-rich components. Usually, metals are vented during explosive events, but sometimes the mixture ascends from the magma chamber and can be injected upward through collapse-related fissures or secondary craters on stratovolcano's flanks. Then, the melt rich in metal crystals and gas forms massive ore bodies and breccia at depth and the surface lava-like flows and pyroclastic deposits enriched in magnetite, hematite, and other metals. Then, the difference in color confirms that Unit A is associated to Cuicocha dome collapse, and is the first insight of possible metal-rich formations in a hydrothermal system in CCVC (Ovalle et al. 2018).

The gas pipes structures are restricted to Unit A, and the border of Unit A and B. Gas pipes are developed by elutriation. The gas in the hot recently deposited material tries to escape through the non-compacted deposit forming the gas pipes. Then, we can assimilate that the emplacement temperature was high enough to develop the pipes in pyroclastic flow in A and the base of Unit B surge. The occurrence of gas pipes reveals in situ formation within the promptly aggrading deposit.

The set of faults recognized in Figure 22 has origin in local stresses associated with a large system of quaternary Billecocha – Huayrapungo faults in the study zone. The local system has a NE-SW orientation, determined by the cinematic of the North Andes (Almeida, 2014). Nevertheless, the lack of exposition of faults and related features, and the objectives in this work do not allow a more deep interpretation.

The findings in this work can be better interpreted when looking at the vertical variation inside both units A and C with a characteristic facies mLA. The results show few variations along with the thickness in both Unit A and C. Both units share cyclicity in both statistical parameters of particle size and component fraction. Then, it is natural to think that both units have a common origin; this is a concentrate PDC, as demonstrated by the granulometry in Figure 29 that based on the poorly sorting in the fine sand size establish as parental current a concentrated pyroclastic flow.

6.2 Comparison with previous works

This study was carried out in quarries with a high rate of change restricted to the medial zone. Then, the correlated unit in this section has some differences related to the detail level in the construction of stratigraphic columns and the extension of studied areas. Von Hillebrandt (1989) has performed a detailed stratigraphic reconstruction in 13 columns that cover a broad area around the caldera, and Pidgen (2014) states a summary of the stratigraphic relations in a compound column with three central units in an area 4km around the caldera. However, Pidgen (2014) is away from establishing a detailed analysis of the stratigraphy.

The findings here agree with previous descriptions of Hillebrandt (1989) and partially match with Pidgen (2014). Although the correlation between our stratigraphy and those of previous authors is complicated, I am confident that the correlation presented in figure 30 is coherent with the shreds of evidence verified in field campaigns. Figure 30 matches units A, B, and C in this work with unit C in von Hillebrandt's. Over the first massive unit, this work and Hillebrandt (1989) establish a well-bedded sequence. Meanwhile, this bedded deposit define Unit B by itself in this work, for Hillebrandt this stratified layer represents a volume of rock inside her Unit C. Finally, Hillebrandt state a massive unit over the central bedded layer that is appropriated correlated with Unit C in this work. The last meter in Hillebrand work corresponds to a stratified set of rocks that do was not found in the studied area are, and thus there is no correlation of the new surge deposit over the last pyroclastic flow in Unit C. The stratigraphy in Pidgen (2014) did not present a pertinent unit to correlate in the base of the column. Then, Pidgen has identified the youngest of the pyroclastic flows and an overlying surge deposit that Hillebrandt draws to finish the sequence. This correlation states that Pidgen (2014) has not identified nor the stratified layer related to Unit B in this work neither unit A.

The differences can be related to the studied areas, and the proximity f studied outcrops to the caldera. Then, the upper surge is not present at a middle distance and possible is restricted to the proximal area to the caldera.

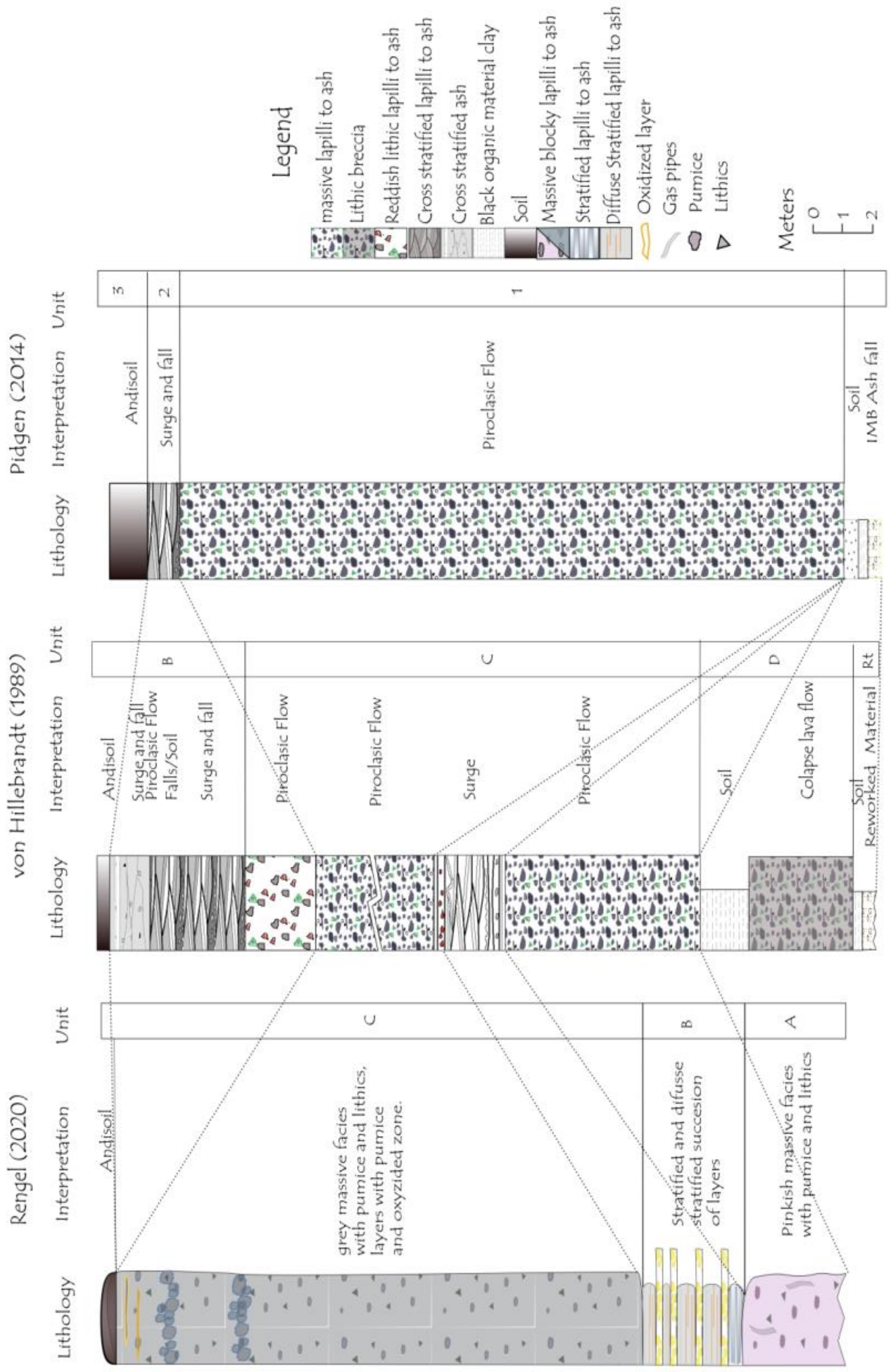

Fig. 29 Stratigraphic correlation with previous work.

6.3 Granulometry and Vertical variation statistical parameters and components.

Fourteen samples at different levels in Unit A and C, as shown in Figure 31, were analyzed for granulometry, statistical parameters of particle size, and components. The histograms for granulometry reflect unimodal tendency with a peak between 1φ and 3φ like in sample Cui 13 in figure 23, but also bimodal behavior that represents the content of coarse lapilli and pebble clast of both pumice and lithics. This double peak is consistent with the observations in the field, where the massive deposits have a fine matrix with abundant lithic and pumices coarse clasts. Some histograms that do not present the double peak represent a sample that did not include the coarse clast in the sample.

The statistical analysis that compares sorting and the median grain size in fig 29 ensures that the deposits correspond to a pyroclastic flow, as described by Walker (1971). According to Branney & Kokelaar (2002), four factors contribute to poor sorting. First, the rapid decompression of magma, vesicle rupture, and the dispersion of the product by the eruptive column create a diverse size in grains from bombs to fine ash. Second, the explosive fragmentation processes and the chaotic mixing create a very poorly sorted grain-size population with abundant fine ash like the studied deposits. The different sizes and proportions of components are justified by the origin and transport of the material. Third, it takes just seconds to minutes from the formation of the clasts in an eruptive eruption to the time of deposition. Then, the segregation processes (i.e., elutriation of ash) occur rapidly without enough time to sort the clasts. Finally, four the attrition of pumice clasts during the transport could produce fine ash. Attrition is the combination of the breakage of large particles and abrasion; both add fine ash into the current. The evidence in this phenomenon is the rounding of pumice lapilli, and the subangular lithics have been deformed during the transport, and the broken part becomes part of the current by attrition what increasing the fine components in the current as presented in the ternary diagram in Figure 25.

Figure 31 shows variations of statistical parameters (Md, sorting, Sk, and KG) and components along with the thickness. The average Md measure (for both units) is 0.87, which is represented by a red line in the box. The values in Unit A of Md start smaller than the average while the second and third are higher than the average. The second value corresponds to Cui 8 and is the biggest among all the samples with a value of 2.02 associated with a finer sand matrix (than the average) and a lack of coarse clasts in the sample. Meanwhile, Md in Unit C fluctuates around the average with a tendency to remain smaller than the average or have more coarse sand material, indicating coarser clast in the analyzed samples. The sorting remains in the area of very poorly sorted material (>2) for all the samples. The Sk is negative in Unit A and unit C. Both Units present constant change between more symmetrical to negative Sk. The unimodal sample that does not include coarser clasts is more symmetrical, while the samples that have two peaks are less symmetrical, with a tendency to negative Sk. KG is leptokurtic in all the thickness for Unit A and fluctuates between mesokurtic (0.9 to 1.11) values and leptokurtic (1.11 to 1.50) values for Unit C, which is the consequence of the predominance of coarse ash (Fig 25, and 28). The stratigraphy revealed some cyclicity and few significant

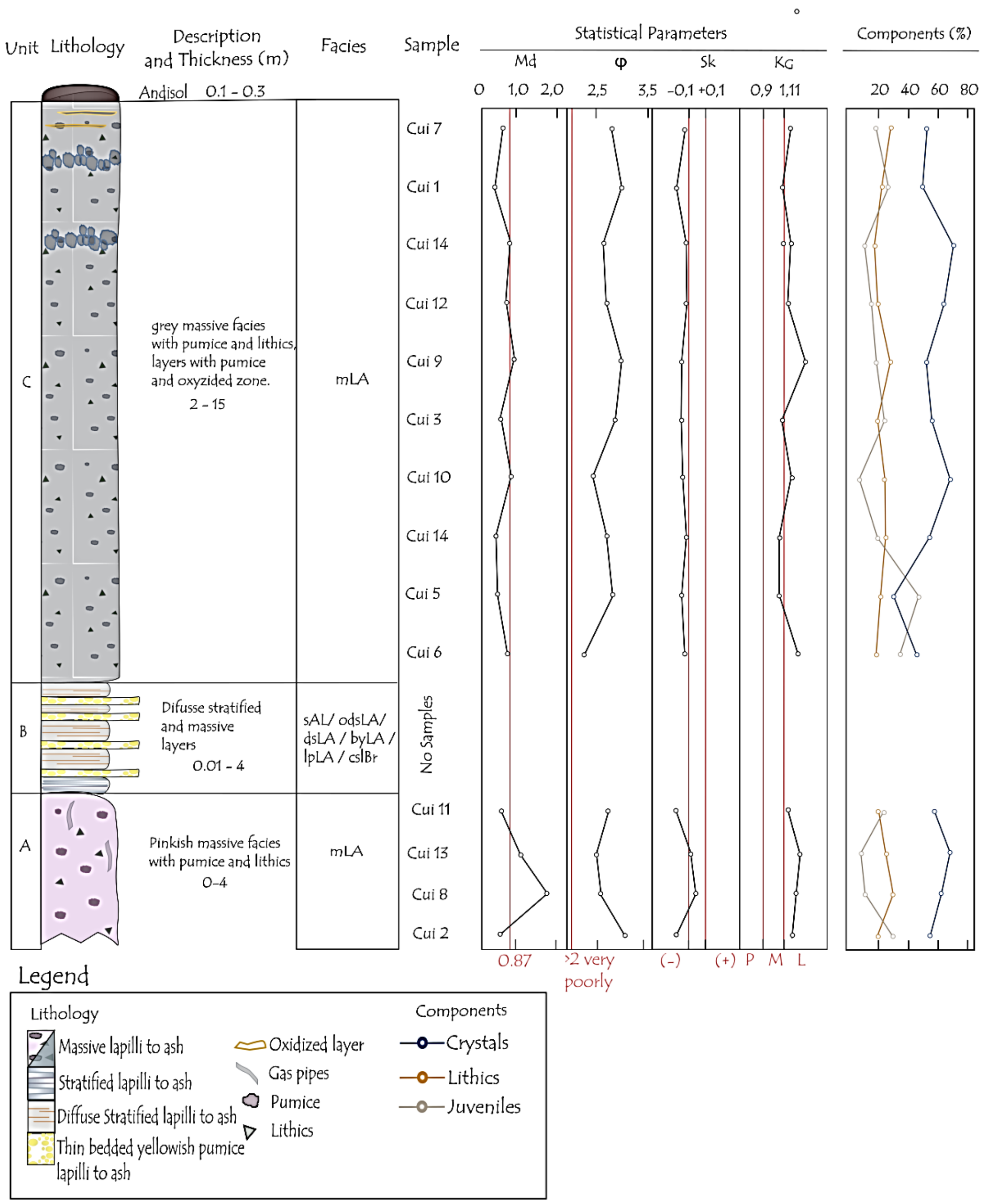

Fig. 30 Vertical changes in the statistical parameters of particle size distributions and components.

variations in the statistical parameters associated to an unsteady parental current and its turbulent motion.

I want to discuss the vertical trends in the components: lithics, juveniles, and crystals. The lithics vary around 20% for both units A and C without big disparities. Besides, juveniles and crystals follow opposite trends. This means when one increases, the other decreases and vice versa. Unit A decreases in juveniles in the base of the outcropping sections and increases in crystals to the top. Then, at the begging of Unit C, the juveniles increase to the maximum value measured by 50%, and the crystal decreases to the lower value measured by 30%. The content of juveniles decreases to the lowest quantity, and the crystal goes up to 70%. Afterward, the cycle increases and decreases one more time, and the sequence finishes 20% for juveniles and 60% for crystals.

In particular, the origin of the lithic class in the facies can be accredited to collapse from the eruption conduit, and the erosion from substrates or the lithics can be included in the current as accidentals fragments. No hydrothermal alterations like chemical alteration (metasomatism) typical of the conduit or magma chamber were found. In this case, most probably, the lithic were part of the dome and were added to the current and transported. The juvenile's content comes from fresh magma erupted in the explosion and quenched fast, and as well the crystals (fragments) come from the magma.

The described stratigraphic features granulometry and components are similar to some features from the first eruption of Mount Saint Helens, USA. The first eruption has strongly depleted the magma of its volatile components, and the system in Mount Saint Helens did not add new magma to the magma reservoir. As a consequence, the successive eruption and pyroclastic flows were less violent and produces viscous domes, lava flows, and smaller volumes of pyroclastic-flow deposits. This hypothesis can be incorporated into the eruptive history of Cuicocha. Hillebrandt (1989) suggests that the pyroclastic flows in the first eruption are larger than the pyroclastic in the second eruption, and then the rest of magma depleted in volatiles produces the domes inside the caldera, as described by Rowley et al. (1982) for Mount Saint Helens.

Chapter 7: Conclusion and recommendations

7.1 Conclusion

The PDC deposits are essential to understand the Cuicocha eruptive history, which is the youngest volcanism in the studied zone and nowadays presents signs of active activity as seismicity and degasification. The findings show two PDC distributed predominantly to the southeast of the current caldera and extended several km in this direction. The understanding of these deposits supposes some insight to understand the parental current and, therefore, the eruptive behavior of Cuicocha.

The present work describes the physical characteristics of PDC's from Cuicocha caldera, the lateral variation in the defined units, and the vertical variation in facies, components, and statistical parameters to understand their genesis and depositional mechanisms. The thesis work has compiled information available about the eruptive history and volcanic products in Cuicocha. Furthermore, I provide new stratigraphic columns, granulometry, and components information of the pyroclastic deposits and relate those to the eruptive stages of Cuicocha caldera volcano.

The eruptive history of Cuicocha can be shortly summarized in the following stages. First, the Cuicocha dome growth on the southeastern flank of Cotacachi Volcano. After two significant eruptions took place, one destroys Cuicocha dome, and the other represented a reactivation of CCVC. Both originated substantial volumes of PDC that are the main object of study in this work. Finally, four domes grow inside the caldera.

The findings in this study clearly show that the two main eruptive processes of Cuicocha can be recognized by two ignimbrites. The first is characterized by a pinkish massive deposit unit A, which base has not been found, and its maximum thickness exposed is 4 m. The literature review state that this deposit has 4.1 km^3 and is the most prominent current in terms of volume. The second event is characterized by two units B, and C. Unit B is a stratified unit of variable thickness 0.01 to 4m in contact with the upper limit in unit A. Overlying the sequence a massive grey unit C with thickness up to 15m in its maximum and a volume of 0.8 km^3.

The lithofacies description and interpretation allows the understanding of the transport and deposition process. Massive ignimbrite corresponds with Cuicocha units A and C that were deposited by a concentrated steady flow progressively aggraded. Unit B is a stratified unit with a well-developed process of segregation in an unsteady and steady flow of primary and secondary origin deposited by progressive aggradation. The massive ignimbrites are a consequence of a concentrated PDC, while the stratified layer comes from a surge or dilute PDC, both are end members of the current spectrum.

The parental current determines the characteristics of different lithofacies than can vary with time (vertically) and space (horizontally) as demonstrated by the variation in columns and the vertical sequences in each in the relatively short study area. Thus, the horizontal variations in the units record changes in the distribution of the current over the area, and the vertical arrangement of lithofacies in a specific side is consequence of the unsteadiness in the current.

Finally, this work has joined the knowledge exposed in Hillebrandt (1989) and Pidgen (2014) to be compared with original finding in the field located at media distance and laboratory (granulometry and component analysis) to corroborate the stratigraphy at a middle distance from the caldera and the origin of the found ignimbrites. Equally important, the different samples support the understanding of vertical and horizontal changes in the current. Cuicocha caldera is still a big unknown for the volcanologist all around the work, and the description in this work should consider part of the fundaments for future studies.

7.2 Recommendations

The following recommendations could be taken into account for a further job based on what I learned by developing this thesis work and was out the limits of this study.

The distribution of outcrops does not allow an evaluation of changes from proximal to the distal sites to the caldera. Therefore, new studies about the changes in the current with base in proximal to distal deposit. This type of study can provide insights into changes of current along the flank of deposition. The river ravines close to our study locations were not studied. Nonetheless, it is crucial to consider that they can expose the units in more proximal and distal points.

The studies of the ignimbrites implicate a detailed analysis of the distribution, the internal arrangement of lithofacies, thickness variations/bed, bounding surfaces, and the relations of these features to topography and characteristics of the substrate could define the transport and deposition of the PDC. Any further study of parameters like paleorelief, sedimentation rates, elutriation, clast abrasion and breakage, interaction with the substrate, and air ingestion would explain better the eruptive history of Cuicocha. Also, a work that reveals trends of lineation and grain fabrics (e.g., imbricated pumices) of clast in the deposits can allow us to support an interpretation of the stresses within the flow-boundary zones of the PDC. Moreover, it could be useful to take into account ferromagnetic minerals in grains and clast at the massive facies because those could register the magnetism in rocks. The remnants of magnetism could give insights about the temperature of the deposition of the current.

Even though we know the location and geometry of Cuicocha caldera, the kinematics, tectonic setting of the main caldera structure, and its development are poorly known. Moreover, Hall et al. (1999) state that sector collapses tend to occur perpendicular to regional faults. There is a critical fault system going through CCVC that could be better understood through structural studies. Cuicocha caldera could be closely related to these faults, as suggested by Acocella (2007).

Also important, Cuicocha dome is a big unknown still. Any attempt to reconstruct the previous Cuicocha dome in its size, volume, and estimate its rate of growth would add significantly to the understanding and knowledge about Cuicocha of the volcanism at CCVC.

Regarding the age, just von Hillebrandt (1989) has proposed a range of times in which the CFE and the second reactivation of the Cuicocha the age suggested by radiocarbon suggest 3.1 ka ±0.15 and 2.9 ka ± 0.15 as consider in this work. Nevertheless, Pidgen suggests that the gap between the events could be tens of years, which is consistent with our observations that paleo soil layers are absent between Units 1 and 2. New age datation analysis could improve the accuracy in the dates.

.

References

Acocella, V. (2007). Understanding caldera structure and development: An overview of analog models compared to natural calderas. *Earth-Science Reviews*, *85*(3-4), 125-160.

Acocella, V., Di Lorenzo, R., Newhall, C., & Scandone, R. (2015). An overview of recent (1988 to 2014) caldera unrest: Knowledge and perspectives. *Reviews of Geophysics*, *53*(3), 896-955.

Almeida, M. (2016). *Estudio Petrográfico y Geoquímico del volcán Cotacachi, provincia de Imbabura* (Tesis de ingeniero geólogo). Escuela Politécnica Nacional, Quito-Ecuador).

Branney, M. J., Kokelaar, P., & Kokelaar, B. P. (2002). *Pyroclastic density currents and the sedimentation of ignimbrites.* Geological Society of London.

Cadena A. (2020) Dirección Provincial de Ambiente de Imbabura. 2020

Cas, R., & Wright, J. (2012). Volcanic successions modern and ancient: A geological approach to processes, products and successions. Springer Science & Business Media.

Cashman, K. V., & Giordano, G. (2014). Calderas and magma reservoirs. *Journal of Volcanology and Geothermal Research*, *288*, 28-45.

Córdova A., Villarreal E., & Ruiz M. (2019). Informe Mensual del Complejo Volcánico Cotacachi - Cuicocha Febrero – 2019. Retrieved December, 2019 from: https://www.igepn.edu.ec/cuicocha-informes/cui-mensuales/cui-m-2019

Córdova A., Villarreal E., & Ruiz M. (2019). Informe Mensual del Complejo Volcánico Cotacachi - Cuicocha Enero – 2019. Retrieved December, 2019 from: https://www.igepn.edu.ec/cuicocha-informes/cui-mensuales/cui-m-2019

Córdova A., Villarreal E., Proaño A., & Ruiz M. (2019). Informe Mensual del Complejo Volcánico Cotacachi - Cuicocha Segundo Trimestre – 2019. Retrieved December, 2019 from: https://www.igepn.edu.ec/cuicocha-informes/cui-trimestrales/cui-t-2019

Córdova A., Villarreal E., Proaño A., & Ruiz M. (2019). Informe Mensual del Complejo Volcánico Cotacachi - Cuicocha Primer Trimestre – 2019. Retrieved December, 2019 from: https://www.igepn.edu.ec/cuicocha-informes/cui-trimestrales/cui-t-2019

December 2019)

Druitt, T. H., & Sparks, R. S. J. (1984). On the formation of calderas during ignimbrite eruptions. *Nature*, *310*(5979), 679.

Giles D.L. (1968) Graben. In: Geomorphology. Encyclopedia of Earth Science. Springer, Berlin, Heidelberg

Global Geoparks Network. (n.d.). *What is a UNESCO Global Geopark?* Retrieved December 18, 2019 from http://www.globalgeopark.org/aboutGGN/6398.htm

Gunkel, G. & Beulker C. (2009). Limnology of the Crater Lake Cuicocha, Ecuador, a Cold Water Tropical Lake. *International Review of Hydrobiology*, 94(1), 103-125.

Hall, M. L., Samaniego, P., Le Pennec, J. L., & Johnson, J. B. (2008). Ecuadorian Andes volcanism: A review of Late Pliocene to present activity. *Journal of Volcanology and Geothermal Research*, *176*(1), 1-6.

Instituto Geofísico de la Escuela Politécnica Nacional. (n.d.). *Cotacachi – Cuicocha*. Retrieved December 18, 2019, from https://www.igepn.edu.ec/cuicocha

Iriondo, Martín & Kröhling, Daniela. (2007). Non-classical types of loess. Sedimentary Geology. 202. 352-368. 10.1016/j.sedgeo.2007.03.012.

Mueller, S., Scheu, B., Kueppers, U., Spieler, O., Richard, D., & Dingwell, D. B. (2011). The porosity of pyroclasts as an indicator of volcanic explosivity. *Journal of Volcanology and Geothermal Research*, *203*(3-4), 168-174.

Natural Resources Conservation Service. (n.d.). Retrieved March 20, 2020, from https://www.nrcs.usda.gov/wps/portal/nrcs/detail/wa/soils/?cid=nrcs144p2_036333

Nichols, G. (2009). *Sedimentology and stratigraphy*. John Wiley & Sons.

Ovalle, J.T., La Cruz, N.L., Reich, M. *et al.* Formation of massive iron deposits linked to explosive volcanic eruptions. *Sci Rep* **8,** 14855 (2018). https://doi.org/10.1038/s41598-018-33206-3

Pardo Villacreces, N. (2012). *Andesitic Plinian eruptions at Mt. Ruapehu (New Zealand): from lithofacies to eruption dynamics: a thesis presented in partial fulfillment of the requirements for the degree of Doctor of Philosophy in Earth Science at Massey University, (Palmerston North, Manawatu), New Zealand (Doctoral dissertation, Massey University).*

Pidgen, A. (2014). Cuicocha Volcano, Ecuador: reconstruction of major explosive phases through investigation of associated pyroclastic deposits (Unpublished master´s thesis). University of Oxford, Oxford, United Kingdom.

Roduit, N. JMicroVision: Image analysis toolbox for measuring and quantifying components of high-definition images. Version 1.3.1. https://jmicrovision.github.io (accessed

Roverato, M., & Capra, L. (2013). Características microtexturales como indicadores del transporte y emplazamiento de dos depósitos de avalancha de escombros del Volcán de Colima (México). Revista mexicana de ciencias geológicas, 30(3), 512-525.

Roverato, M., Capra, L., Sulpizio, R., & Norini, G. (2011). Stratigraphic reconstruction of two debris avalanche deposits at Colima Volcano (Mexico): insights into pre-failure conditions and climate influence. Journal of Volcanology and Geothermal Research, 207(1-2), 33-46.

Kuntz, M., Rowley, P., Norman, S., Reynolds R., McBroome, L., Kaplan A., & Lidke D. (1982). *The 1980 eruptions of Mount St. Helens, Washington. Pyroclastic Flows.* (Vol. 1250). US Department of the Interior, US Geological Survey.

Rowley, P., Kuntz, M. & Macleod, N. (1982). *The 1980 eruptions of Mount St. Helens, Washington. Pyroclastic Flows.* (Vol. 1250). US Department of the Interior, US Geological Survey.

Sigurdsson, H., Houghton, B., McNutt, S., Rymer, H., & Stix, J. (Eds.). (2015). *The encyclopedia of volcanoes*. Elsevier.

Sulpizio, R., & Dellino, P. (2008). Sedimentology, depositional mechanisms and pulsating behavior of pyroclastic density currents. *Developments in Volcanology, 10*, 57-96.

Sulpizio, R., Dellino, P., Doronzo, D. M., & Sarocchi, D. (2014). Pyroclastic density currents: state of the art and perspectives. *Journal of Volcanology and Geothermal Research*, *283*, 36-65.

United Nations Educational, Scientific and Cultural Organization. (2019). Gallery: Imbabura UNESCO Global Geopark Ecuador.

Von Hillebrandt, C. (1989). ESTUDIO GEOVULCANICO DEL COMPLEJO VOLCANICO CUICOCHA-COTACACHI Y SUS APLICACIONES, PROVINCIA DE IMBABURA (Unpublish master´s thesis). Escuela Politécnica Nacional, Quito, Ecuador.

Walker, G. P. (1971). Grain-size characteristics of pyroclastic deposits. *The Journal of Geology*, *79*(6), 696-714.

Walker, G. P. (1983). Ignimbrite types and ignimbrite problems. *Journal of volcanology and geothermal research*, *17*(1-4), 65-88.

Wills, B. A., & Finch, J. (2015). Wills' mineral processing technology: an introduction to the practical aspects of ore treatment and mineral recovery. Butterworth-Heinemann.

Wright, J. V., Smith, A. L., & Self, S. (1981). A terminology for pyroclastic deposits. In Tephra Studies (pp. 457-463). Springer, Dordrecht.

Epílogo

Esta tesis de grado se terminó en medio del inicio de una pandemia sin precedentes en el planeta Tierra y con consecuencias más que fatales en muchos países incluyendo mi Ecuador. Las personas (que podemos) nos mantenemos en casa. Sin embargo, afuera en las calles de las ciudades más grandes como Guayaquil y Quito cientos de personas mueren en busca de atención medica en centros de salud colapsados. Nadie se ha salvado de esta pandemia y tampoco de la corrupción de las autoridades.

Esperemos que el futuro no sea tan malo como es el presente y que los/las estudiantes ecuatorianos y en especial las/los estudiantes de Yachay Tech logremos hacer que nuestro país no vuelva a ser un objeto pisoteado hasta el cansancio por políticos corruptos como los del gobierno de Lenin Moreno.